Journal of Hydrology 569 (2019) 203–217

Contents lists available at ScienceDirect

Journal of Hydrology

journal homepage: www.elsevier.com/locate/jhydrol

Research papers

Climatic or regionally induced by humans? Tracing hydro-climatic and land-use changes to better understand the Lake Urmia tragedy

Bahram Khazaei[a,*], Sina Khatami[b], Seyed Hamed Alemohammad[c], Lida Rashidi[d], Changshan Wu[e], Kaveh Madani[f,g], Zahra Kalantari[g], Georgia Destouni[g], Amir Aghakouchak[h,i]

[a] Department of Civil and Environmental Engineering, University of Wisconsin-Milwaukee, USA
[b] Department of Infrastructure Engineering, University of Melbourne, Australia
[c] Radiant.Earth, USA
[d] Department of Computing and Information Systems, University of Melbourne, Australia
[e] Department of Geography, University of Wisconsin-Milwaukee, USA
[f] Centre for Environmental Policy, Imperial College London, UK
[g] Department of Physical Geography and Bolin Centre for Climate Research, Stockholm University, Sweden
[h] Department of Civil and Environmental Engineering, University of California, Irvine, USA
[i] Department of Earth System Science, University of California, Irvine, USA

ARTICLE INFO

This manuscript was handled by Andras Bardossy, Editor-in-Chief, with the assistance of Roger Moussa, Associate Editor

Keywords:
Lake Urmia
Climate change
Land-use change
Anthropogenic change
Vegetation
Water resources management

ABSTRACT

Lake Urmia—a shallow endemic hypersaline lake in northwest Iran—has undergone a dramatic decline in its water level (WL), by about 8 m, since 1995. The primary cause of the WL decline in Lake Urmia has been debated in the scientific literature, regarding whether it has been predominantly driven by atmospheric climate change or by human activities in the watershed landscape. Using available climate, hydrological, and vegetation data for the period 1981–2015, this study analyzes and aims to explain the lake desiccation based on other observed hydro-climatic and vegetation changes in the Lake Urmia watershed and classical exploratory statistical methods. The analysis accounts for the relationships between atmospheric climate change (precipitation P, temperature T), and hydrological (soil moisture SM, and WL) and vegetation cover (VC; including agricultural crops and other vegetation) changes in the landscape. Results show that P, T, and SM changes cannot explain the sharp decline in lake WL since 2000. Instead, the agricultural increase of VC in the watershed correlates well with the lake WL change, indicating this human-driven VC and associated irrigation expansion as the dominant human driver of the Lake Urmia desiccation. Specifically, the greater transpiration from the expanded and increasingly irrigated agricultural crops implies increased total evapotranspiration and associated consumptive use of water (inherently related to the irrigation and water diversion and storage developments in the watershed). Thereby the runoff from the watershed into the lake has decreased, and the remaining smaller inflow to the lake has been insufficient for keeping up the previous lake WL, causing the observed WL drop to current conditions.

1. Introduction

The observed climatic changes during the past decades (IPCC, 2014, p. 30) have impacted most physical and natural processes on Earth, including the hydrological cycle, vegetation, and ecological balance of ecosystems (Baldwin et al., 2001; House et al., 2016; Piao et al., 2006). In addition, extreme climate events are expected to intensify, with increasing impacts on human life (Golian et al., 2015; Pachauri and Meyer, 2014; Vörösmarty et al., 2010). However, some of the global environmental changes, including those in water resources systems at the Earth's surface (Pokhrel et al., 2017) and subsurface (Felfelani et al., 2017; Hashemi et al., 2015; Mohan et al., 2018)—such as rivers, streams, lakes, and groundwater—may also be due to human-driven land- and water-use developments and changes in the landscape itself (Destouni et al., 2013, 2010, Jaramillo and Destouni, 2015, 2014).

In many parts of the world human activities and over-extraction of water beyond what is naturally available have intensified regional droughts; causing a socio-environmental phenomenon known as *Anthropogenic Drought* (AghaKouchak et al., 2015a; Mehran et al., 2017) or *Water Bankruptcy* (Madani et al., 2016). Significant manifestations of such human-induced droughts can be found in arid and semi-arid regions such as the Middle East (Al-Damkhi et al., 2009; Bari Abarghouei

* Corresponding author.

https://doi.org/10.1016/j.jhydrol.2018.12.004
Received 1 March 2018; Received in revised form 3 November 2018; Accepted 4 December 2018
Available online 07 December 2018

et al., 2011; Berndtsson et al., 2016; Davtalab et al., 2017, 2014; Gohari et al., 2013; Golian et al., 2015; Hashemi, 2015; Izady et al., 2012; Madani, 2014; Mehran et al., 2015).

Lake Urmia, a major hypersaline lake, is a prime example of an environmental tragedy in Middle East (Karbassi et al., 2010; Khatami and Berndtsson, 2013; UNEP & GEAS, 2012), where both climatic and anthropogenic changes might be significant (Alborzi et al., 2018; Jamali et al., 2013; Rodell et al., 2018). The surface area of the lake has decreased dramatically, by around 88%, during the past two decades (AghaKouchak et al., 2015b; Jalili et al., 2015). Due to its unique ecosystem and the extent of its deterioration, the fate of Lake Urmia has become an active but controversial research topic in recent years. Various aspects of the lake, including the dominant causes of its desiccation, have been studied from different standpoints, leading to a contested debate between two main camps.

While some researchers consider the Lake Urmia retreat to be *predominantly* the outcome of the changing climate and a climate-driven increase of droughts (Delju et al., 2013; Fathian et al., 2015) others argue that, similarly to other parts of the world (Destouni et al., 2013; Jaramillo and Destouni, 2015, 2014), the lake may be suffering from *Aral Sea Syndrome* (AghaKouchak et al., 2015b) implying that its current situation is not primarily due to purely atmospheric climate change. Although seasonal changes in the lake water level are strongly influenced by large-scale atmospheric circulation patterns (Jalili et al., 2012) different studies have attributed the decline in lake water content to extensive human activities in the watershed itself, such as various dam building projects, especially since the 1990s (Alborzi et al., 2018; Ashraf et al., 2017; Hassanzadeh et al., 2012; Khatami, 2013, p. 82; Khoshtinat et al., 2015; Khosravi et al., 2018), groundwater over-exploitation at rates faster than the aquifer recharge rate (Alizade Govarchin Ghale et al., 2018; Amiri et al., 2017, 2016; Ashraf et al., 2017; Khatami, 2013, p. 16; Tourian et al., 2015; Vaheddoost and Aksoy, 2017), causeway construction (Marjani and Jamali, 2014; Zeinoddini et al., 2009), expansion of irrigated agriculture (Khazaei et al., 2016; Mehrian et al., 2016), and over-consumption of irrigation water through inefficient agricultural practices (Stone, 2015; Torabi Haghighi et al., 2018). The last two drivers of water change, i.e., the agricultural and irrigation expansions in the Lake Urmia watershed, imply increased water demands that are positively linked with the other change drivers such as expansion of water storage capacity through extensive dam building and groundwater over-exploitation (Madani, 2014; Mesgaran et al., 2017) in the same watershed. In addition, there is consensus among most researchers that the lake's situation has been exacerbated by frequent droughts reducing the total available natural water budget of the lake and its watershed (Alborzi et al., 2018; Farajzadeh et al., 2014; Khalyani et al., 2014).

Lake Urmia is a prime example of growing number of lake desiccation cases due to Aral Sea Syndrome occurrence seen in various parts of the world. Thus, this study develops a change-attribution approach (Section 3.4. Change-Attribution Approach) to evaluating the significance of different climatic and anthropogenic (landscape) change drivers over the Lake Urmia watershed for the change impacts observed in the watershed vegetation (including agricultural crops and other vegetation) and in Lake Urmia itself (Section 4. Results and Discussions). The vegetation development is thus investigated as a possible important impact indicator of the hydro-climatic interplay between the atmospheric climate change and the hydrological and various agriculture-related human developments occurring over the watershed landscape. The study involves a statistical analysis of climate, hydrological, and vegetation characteristics for the period 1981–2015. For this period, we compile the available data and compare the variations and long-term patterns of the atmospheric climate variables of land surface air temperature (T) and precipitation (P), the hydrological variables of soil moisture (SM) and lake water level (WL) and a vegetation coverage (VC) variable for the landscape of the Lake Urmia watershed. For these main hydro-climatic-vegetation variables (T, P, SM, WL, and VC), an integrated correlation and trend analysis is conducted, using monthly and seasonal data for 2000–2015. The developed approach in this study can be applied for better investigation of similar cases around the world.

Fig. 1. Map of the Lake Urmia watershed and its location in Iran (Natural Earth Map Data).

2. Study area and data

2.1. Study area

Lake Urmia is a transboundary water system. The lake itself is located between East Azerbaijan and West Azerbaijan Provinces in northwest Iran (Fig. 1) with inflowing rivers originating in these two provinces and the Kurdistan Province to the south. The lake watershed area is 51,867 km^2 and contains 14 main inflowing rivers (Khatami, 2013). Lake Urmia is a shallow terminal lake with depth varying from 5 to 16 m, length in the S-N direction of approximately 140 km, and central point coordinates of 37°42′ N, 45°19′ E.

The lake is located in a semi-arid climate with mean annual P of about 357 mm (Fazel et al., 2017; Khalyani et al., 2014; Vaheddoost and Aksoy, 2017), and the mean annual T of about 11 °C (Delju et al., 2013). Daily minimum T in the region ranges between 0 °C and –23 °C in winter, and the daily maximum T can reach 39°C during summers.

Based on measurements made at hydrometric stations located at the outlet of major reservoirs in the watershed, the average water discharge into the lake decreased from 2112 to 750 MCM (million cubic meters)—i.e., around 65% reduction—between 1960 and 2010 (Khoshtinat et al., 2015). The WL of the lake has also dropped significantly in recent decades from 1278 m above sea level (m.a.s.l) in 1995 to 1270 m.a.s.l (water depth reduction of ~8 m) in 2014 (Khatami and Berndtsson, 2012; Tourian et al., 2015; Zoljoodi and Didevarasl, 2014).

2.2. Climate data

Climatic conditions in the Lake Urmia watershed are assessed in terms of the main climate variables P and T, which generally have significant implications for the hydrologic cycle and vegetation dynamics.

2.2.1. Precipitation

Three datasets are used here to analyze monthly P (Fig. 2). These are: the Climate Prediction Center (CPC) Merged Analysis of

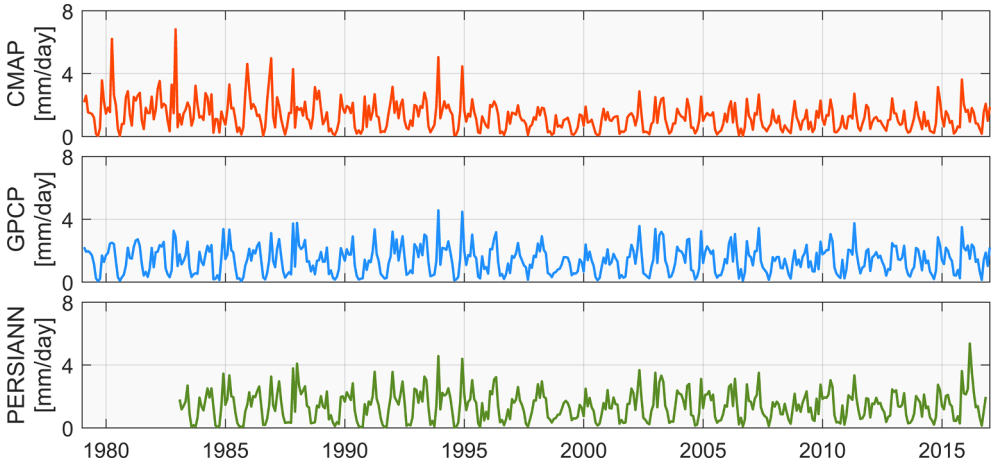

Fig. 2. Mean monthly time series of precipitation (P) in the Lake Urmia watershed, based on the CMAP (top), GPCP (middle), and PERSIANN-CDR (bottom) datasets.

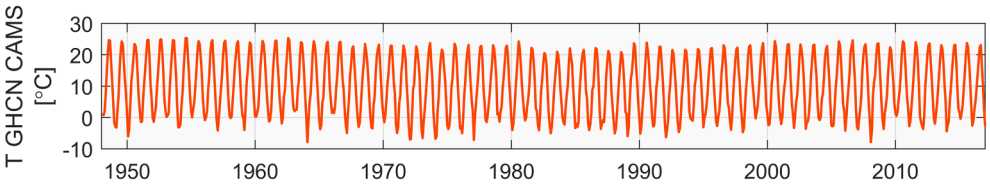

Fig. 3. Mean monthly time series of land surface air temperature (T) in the Lake Urmia watershed, based on the GHCN CAMS dataset.

Precipitation (CMAP); the Global Precipitation Climatology Project Version 2.3 (GPCP); and the Precipitation Estimation from Remotely Sensed Information using Artificial Neural Networks – Climate Data Record (PERSIANN-CDR).

CMAP is a product of the US National Oceanic and Atmospheric Administration (NOAA) and provides average monthly data from 1979 to present with a spatial resolution of 2.5°×2.5° (NOAA, 2016a). CMAP data are derived from microwave and infrared observations from polar orbiting and geostationary satellites, as well as gauge data analysis. GPCP (Adler et al., 2003) provides data with the same spatial and temporal resolution as CMAP but uses geostationary infrared satellite imagery retrievals and different algorithms to estimate P. PERSIANN-CDR daily mean P data is available from 1983 at a 0.25° × 0.25° spatial resolution. This dataset primarily relies on satellite infrared observations and is corrected based on passive microwave information and ground-based observations (Ashouri et al., 2015).

Overall, the three P data sets are consistent with respect to their mean daily P information. PERSIANN-CDR and GPCP indicate that the average P in the Lake Urmia watershed is 1.4 mm/day, whereas CMAP shows that the average P is 1.3 mm/day.

To select the best P estimate for our study domain, the Triple Collocation (TC) error characterization method (Stoffelen, 1998) is applied to the three P estimates. TC provides an estimate of the random error in three collocated estimates/measurements of the same variable without assuming any of the three to be error-free. TC uses the covariance matrix of the three measurements and by assuming that the three measurements have independent random errors and uncorrelated random errors with the truth, it calculates the variance of the random error in each measurement. In addition, TC also provides the correlation coefficient (CC) between each measurement and the truth. Detailed derivation of this technique is explained in McColl et al. (2014). TC has been applied to a wide range of environmental variables including SM, P, sea surface salinity, and land water storage (Alemohammad et al., 2015; Draper et al., 2013; Parinussa et al., 2011; Ratheesh et al., 2013; Roebeling et al., 2012). The three estimates of P are aggregated to a spatial resolution of 2.5° × 2.5°; and then TC is applied to the aggregated monthly estimates of P between 1983 and 2016, during which all three datasets are available. Tian et al. (2013) assumed the error structure of monthly P data to be additive, based on which the classical Extended Triple Collocation with additive error model (McColl et al., 2014) is used here. The analysis shows that GPCP has the smallest random error among the three, and the highest correlation with the 'truth' based on TC estimates. The standard deviation of random error in GPCP, PERSIANN-CDR, and CMAP is estimated to be 0.04, 0.17, and 0.50 mm/day, respectively; and their respective CCs are 0.99, 0.97, and 0.63. Moreover, GPCP showed the highest correlation with the mean P estimates (derived from the three measurements). Therefore, GPCP is selected as the best data source for the analysis.

2.2.2. Temperature

T data are extracted from another product of NOAA (NOAA, 2016b) representing a combination of the Global Historical Climatology Network (GHCN) and the Climate Anomaly Monitoring System (CAMS) datasets (T GHCN CAMS). This high-resolution dataset provides global monthly T data from 1948 with a spatial resolution of 0.5°×0.5°. It provides T estimates for land areas and is adjusted by comparison with observational data (Fan and van den Dool, 2008). Based on monthly data, the average T in the lake watershed is 9.99°C for the period 1948–2016, while the average T is 10.17°C for the period 2000–2016. The monthly average T time series is presented in Fig. 3.

2.3. Soil moisture data

Surface SM estimates are based on the European Space Agency (ESA) Climate Change Initiative (CCI) program's soil moisture (ESA CCI SM) product. This product blends SM observations from a suite of active and passive instruments and provides a data record of SM estimates for the period 1978–2015 (Liu et al., 2012, 2011; Wagner et al., 2012). Here, the daily data from the latest version (Version 3.2) of this product are used. Observations are aggregated to monthly values for analysis. The spatial resolution of the data is 0.25° × 0.25° (see Fig. 4).

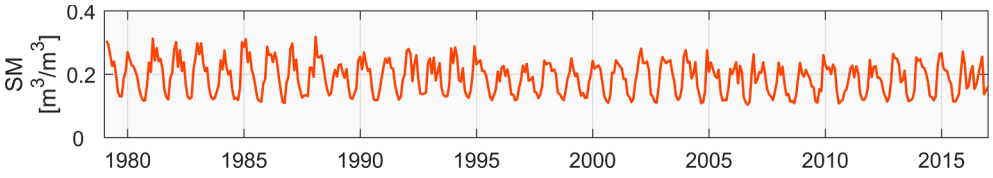

Fig. 4. Mean monthly time series of soil moisture (SM) in the Lake Urmia watershed, based on the ESA CCI SM dataset.

2.4. Vegetation cover data

During recent decades, remote sensing imagery has provided a wide range of tools for monitoring the health and condition of VC, especially for large-scale studies. In this regard, several indices have been defined based on raw remotely sensed reflectance data for study of Earth surface characteristics, among which the normalized difference vegetation index (NDVI) is a useful and well-studied variable for vegetation study (Schultz et al., 2016; Tillack et al., 2014; Viña et al., 2011). NDVI was first used by Rouse et al. (1974) and is calculated based on the response of vegetation to electromagnetic waves in red (RED) and Near-Infrared (NIR) bands:

$$NDVI = \frac{\text{NIR} - \text{RED}}{\text{NIR} + \text{RED}} \quad (1)$$

NDVI is a dimensionless parameter and its value ranges between −1 and 1. Generally, values greater than 0.4 represent temperate and tropical rainforests, while NDVI values between 0.2 and 0.4 indicate grassland. Negative low values near −1 normally refer to water, and small values close to zero (between −0.1 and 0.1) represent urban areas or areas covered by rock, soil, etc. (Weier and Herring, 2000). As suggested by many studies (e.g., Delbart et al., 2005; Khazaei and Wu, 2018; Nemani and Running, 1997), an NDVI value of 0.4 can be used as a threshold for distinguishing vegetation from other types of land cover. This can be used to classify land into vegetated and non-vegetated land cover types and thereby as basis for estimating VC.

In this study, NDVI data are obtained from two US NASA datasets: MOD13Q1 product of MODerate Resolution Imaging Spectrometer (MODIS); and Normalized Difference Vegetation Index-3rd generation using the Global Inventory Monitoring and Modeling System (GIMMS).

MODIS13Q1 is estimated from observations onboard the Terra satellite (Didan, 2015; NASA, 2014a). Since February 2000, MOD13Q1 provides vegetation index values, namely NDVI and enhanced vegetation index (EVI), as well as blue (BLUE), RED, NIR, and Mid-Infrared (MIR) bands on an 8-day basis at a spatial resolution of 250 m. EVI is another commonly used vegetation index that estimates vegetation based on RED, NIR, and BLUE bands with improved sensitivity in highly vegetated areas (Huete et al., 2002). NDVI and EVI products provided by MODIS are computed from atmospherically corrected surface reflectance imagery data, in which water, clouds, heavy aerosols, and cloud shadows have been masked out. Despite its high resolution and abundant temporal availability, MODIS NDVI data is not available prior to the year 2000.

NDVI3g (the latest version of GIMMS product; NASA, 2014b) provides global estimates of NDVI in a daily format with a spatial resolution of 1/12° × 1/12° (~8 km) between July 1981 and 2015 (Pinzon and Tucker, 2014; Tucker et al., 2005). NDVI3g is used for hydro-climatic analyses, including trend and correlation analysis during the 1981–2015 period (see Fig. 5). As MODIS NDVI provides VC estimates with a higher resolution of 250 m, MODIS NDVI is additionally used to evaluate the NDVI3g results on expansion/reduction of VC in the Lake Urmia watershed after February 2000. The evaluation showed that VC estimates of MODIS NDVI and NDVI3g in the Lake Urmia watershed are strongly correlated (CC = 0.92, p-value = 0.00) during the 2000–2015 period.

Any potential trend in net radiation could affect the NDVI estimates (Kustas et al., 1993). Hence, the possible impact of net radiation on the VC estimates is examined over the Lake Urmia watershed. NASA/GEWEX SRB product provides net radiation data globally between 1983 and 2007 (NASA, 2012), and CERES provides net radiation estimates worldwide since 2000 (NASA, 2017). SRB and CERES data were merged to generate net radiation record for the period of 1985–2015 (Orth and Seneviratne, 2015), and no trend was detected in net radiation time series in this period.

2.5. Water level data

Two datasets are used for lake WL: direct gauge observations and the Global Reservoirs/Lakes (G-REALM) dataset.

Daily observations have been recorded at the Golmankhane station (37°36′ N, 45°16′ E) since 1966 (Khatami, 2013, p. 17) and these data were obtained from the Urmia Lake Restoration Program (ULRP). G-REALM also provides WL estimates on a 10-day basis since 1992. G-REALM data are computed from TOPEX/POSEIDON (T/P5), Jason-1, and Jason-2/OSTM altimetry (USDA, 2017). Fig. 6 shows the WL variations of Lake Urmia for the period 1966–2016.

Although observed and remotely sensed WL fluctuations differ as shown in Fig. 6, their trends agree with each other. In this study, gauge observations are selected to analyze WL, since they are on a daily basis and cover a longer period. Additionally, using G-REALM to estimate WL could introduce errors/uncertainties associated with the processing of the satellite data. However, there are also some measurement errors when observed data are used as WL estimates (Khazaei and Hosseini, 2015).

3. Methods

3.1. Point of change detection

A breakpoint towards a rapid decline around the mid-1990s is seen in the WL time series (Fig. 6). The Pettitt test (Pettitt, 1979) is used to find the onset of the WL decline trend and split the WL time series into two shorter periods, before and after the onset, for the further hydro-climatic analyses. The Pettit test is widely used for detecting points of abrupt changes or sharp variations in time series of physical variables (Fan et al., 2012; Rougé et al., 2013; Villarini et al., 2009; Yao et al., 2015). For a given time series of continuous data x_i (i = 1, 2, 3,…, N), the test statistic $U_{t,N}$ is calculated as:

$$U_{t,N} = U_{t-1,N} + V_{t,N}; \quad t = 2, 3, \cdots, N \quad (2)$$

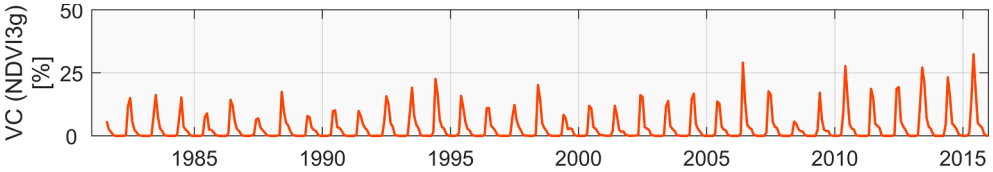

Fig. 5. Mean monthly time series of vegetation coverage (VC) in the Lake Urmia watershed, based on the GIMMS NDVI3g dataset.

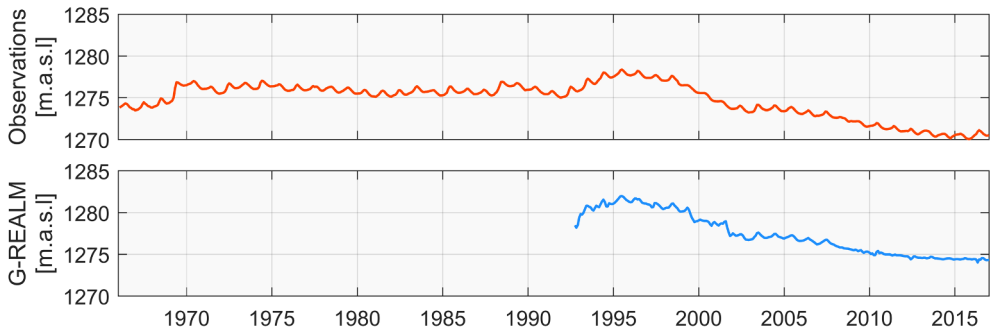

Fig. 6. Mean monthly time series of water level (WL) in Lake Urmia, based on gauge observations (top) and G-REALM data (bottom).

where N is the sample size and

$$V_{t,N} = \sum_{i=1}^{N} sgn(x_t - x_i);\ \ and\ sgn(x_t - x_i) = \begin{cases} 1, & x_t > x_i \\ 0, & x_t = x_i \\ -1, & x_t < x_i \end{cases} \tag{3}$$

The location of the breakpoint K_N in the time series is defined as:

$$K_N = Max\ |U_{t,N}|; \quad t = 1, 2, \cdots, N \tag{4}$$

The statistical significance of K_N can be approximated by:

$$p \cong 2exp\left[\frac{-6K_N^2}{(N^3 + N^2)}\right] \tag{5}$$

For low *p*-values, the null hypothesis "H_0: no change point exists" can be rejected and, there is a significant breakpoint that divides the time series into pre- and post-change parts.

3.2. Trend analysis

3.2.1. Mann-Kendall test

The Mann-Kendall test (Kendall et al., 1990; Mann, 1945) is a nonparametric method for evaluating the presence of a trend or non-stationarity of the mean in a time series and has been widely used to analyze trends in hydrological variables (Ahn and Merwade, 2014; Burn and Hag Elnur, 2002). The test statistics S_{MK} can be defined as:

$$S_{MK} = \sum_{i=1}^{N} \sum_{j=i+1}^{N} sgn(x_j - x_i) \tag{6}$$

where for a time series x_i, i = 1, 2, 3,…, N, the time index i (e.g., the year, month, etc. of observation of each datum) is monotonically increasing by definition, which simplifies the calculations (Wilks, 2011, p. 166). Each and every data point is sequentially treated as a reference point and is compared to all of the following data points (Douglas et al., 2000). The function $sgn(x_j\text{-}x_i)$ is defined in Eq. (3). For N ≥ 8, S_{MK} follows an approximately normal distribution and its variance is calculated as:

$$\sigma_{S_{MK}}^2 = \frac{N(N-1)(2N+5)}{18} \tag{7}$$

The Mann-Kendall test statistic Z_{MK} is calculated by:

$$Z_{MK} = \begin{cases} \frac{(S_{MK}-1)}{\sigma_{S_{MK}}}, & S_{MK} > 0 \\ 0, & S_{MK} = 0 \\ \frac{(S_{MK}+1)}{\sigma_{S_{MK}}}, & S_{MK} < 0 \end{cases} \tag{8}$$

The null hypothesis "H_0: no trend detected" is rejected at 5% significance level (*p*-value < 0.05), when $|Z_{MK}| > 1.96$. Then, a positive value of Z_{MK} indicates a positive trend and a negative Z_{MK} value indicates a negative trend.

3.2.2. Seasonal Kendall trend

The Mann-Kendall test does not account for seasonality and therefore the Kendall seasonal trend method is also used (Hirsch and Slack, 1984). The test statistics are calculated using Equations (9) to (11):

$$S' = \sum_{i=1}^{n_k-1} \sum_{j=i+1}^{n_k} sgn(x_{kj} - x_{ki});\ \ and\ S_{SK} = \sum_{k=1}^{N} S' \tag{9}$$

where j > i, n_k is the count of measurements in season k.

$$\sigma_{S_{SK}}^2 = \sum_{k=1}^{N} \frac{n_k(n_k-1)(2n_k+5)}{18} \tag{10}$$

$$Z_{SK} = \begin{cases} \frac{(S_{SK}-1)}{\sigma_{S_{SK}}}, & S_{SK} > 0 \\ 0, & S_{SK} = 0 \\ \frac{(S_{SK}+1)}{\sigma_{S_{SK}}}, & S_{SK} < 0 \end{cases} \tag{11}$$

As for the Mann-Kendall test, a positive value of Z_{SK} means that the trend is increasing, a negative value signifies a decreasing trend, and zero means no trend. The trend is also significant at *p*-value < 0.05, when $|Z_{SK}| > 1.96$. In the presence of seasonality in the data, the value of Z_{SK} tends to be higher than Z_{MK}.

3.3. Correlation analysis

The association/inter-dependency between different hydro-climatic and vegetation variables is examined using Pearson, Spearman, and Kendall CCs (Bevan, 2013; Kendall and Maurice, 1970). Spearman and Kendall CCs are robust (not dependent upon the underlying distribution of the data) and resistant (not sensitive to extreme values) alternatives to Pearson CC (Wilks, 2011, p. 55). The values of all the above CCs range between −1 and 1. A negative correlation implies an inverse relationship between variables (Ratner, 2009).

3.4. Change-attribution approach

An approach is developed for explaining, i.e., attributing main drivers/causes of the observed water changes, within the classical paradigm of statistical analysis (i.e., frequentist inference). Using an inverse approach, changes in the records (using trend analysis) are first identified, based on which hypotheses are formed to explain the changes. The hypotheses are then evaluated based on observed associations between hydro-climatic variables (using correlation analysis) to explain the changes. Through this approach, the explanatory power of the commonplace exploratory statistical methods is used for change-attribution using the available data for the studied hydro-climatic and vegetation variables, thus constituting a change-attribution analysis. While the spatial variability of each hydro-climatic variable is aggregated into a single representative time series for the whole watershed, the temporal variability is accounted for by performing the analysis across different time scales, namely long-term (defined as the

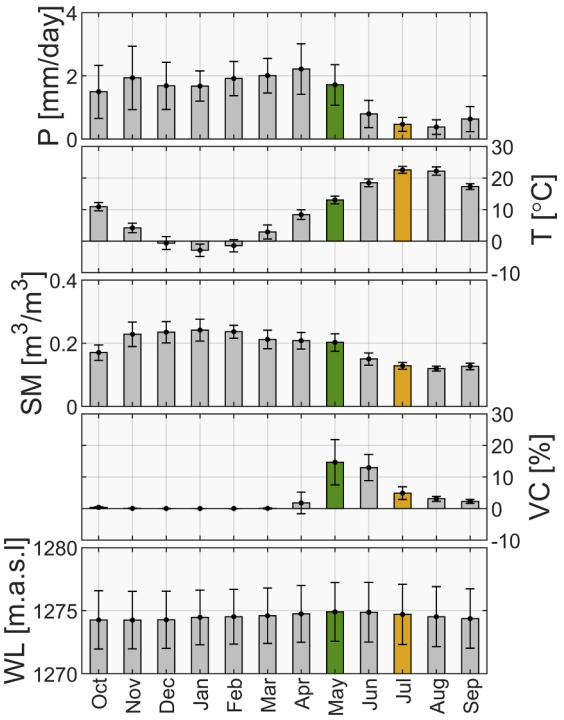

Fig. 7. Monthly average (shaded bars) and the corresponding standard deviation (error bars) of hydro-climatic variables in the Lake Urmia watershed during 1982–2015. May (green) and July (beige) are selected as representatives for wet and dry months. (For interpretation of the references to colour in this figure legend, the reader is referred to the web version of this article.)

entire record) and short-term (defined within each pre- and post-change period), overall (defined over the entire short- or long-term record), and seasonal (defined as wet and dry months in this study for representing intra-annual periods with particular characteristics).

4. Results and discussions

Generating VC data is one of the outcomes of this study, needed for the change-attribution analysis. First, the vegetation dynamics results are presented (Section 4.1), followed by the discussion of the change-attribution analysis results (trends and correlations, Sections 4.2 and 4.3). The section concludes with a discussion of the role of land-water-use changes (i.e., expansion of irrigation and agricultural growth) in the lake's desiccation. The statistically significant results are discussed, although all results (including the non-significant ones) are presented. It should be noted that the statistical significance (i.e., *p*-value) of a given statistic does not necessarily imply its 'importance' or 'size effect'. That is, in interpreting the results, the *p*-value is not a measure of how well (or how much of) the variation in a given variable is associated with the variation in another one (Wasserstein and Lazar, 2016).

4.1. Vegetation dynamics

Fig. 7 shows the monthly average of each hydro-climatic variable based on the common base period for all variables. VC varies considerably in the watershed from spring (April-June) to winter (January-March). The best time of the year for plant growth in the region is late spring and early summer (May-July) when T is moderate and P is maximum (see Fig. 7).

In winter, rainfall amount is sufficient for plant photosynthesis but is mostly in the form of snow, and T is too low that plant photosynthesis is limited. June-September are the hottest months of the year with the least rainfall. VC decreases significantly from May onwards. Fig. 8 further shows the spatial and temporal variations in VC (expressed as NDVI) within the Lake Urmia watershed in April-July during 2000–2016.

Examination of the spatio-temporal dynamics of VC (Fig. 8 and green bars in Fig. 7) suggests that vegetation peaks in May. Based on available observations, average T is estimated to be ~13 °C during this month while P is ~1.7 mm/day, both at proper levels for plant growth. Thus, May is selected as the wet month (spell) representative. July (beige bars in Fig. 7) is also selected as the dry month representative based on its low average P (~0.5 mm/day), maximal average T (~23 °C, i.e., the hottest month of the year), and an expected low average VC. It should be noted that August is also seemingly another candidate for the dry period representative. But the magnitude and variability of VC is very low during August, limiting the analysis of VC change. Spring, particularly May, is an important period for analyzing VC since VC variations (mostly expansion) has occurred at a faster rate during this time.

Vegetation dynamics, expressed as NDVI, are known to be strongly correlated with soil water index and moisture profile (Zribi et al., 2010) and with P (Gessner et al., 2013). Both NDVI and EVI are used here to examine VC. Given their similar results, only those based on NDVI are presented.

4.2. Trends analysis

Trends (magnitude and statistical significance) in the hydro-climatic variables are analyzed across two different sets of time scales; namely (1) short- and long-term periods, and (2) seasonal and overall periods. First, long-term trends in monthly records of the hydro-climatic variables are calculated during 1981–2015 (Fig. 9 and Table 1). Long-term trends may be indicative of climate-driven variations and can provide an overview of the hydro-climatic characteristics of the watershed. Second, short-term trends for the two sub-periods of pre-change (1981–1999) and post-change (2000–2015) are calculated. These sub-periods are defined based on the change point in the WL records, detected as the year 2000 using the Pettitt test. It should be noted that the change point detection method, as a non-parametric analysis, is dependent upon the sample size. That is, selecting the year 2000 as the cut-off for pre- and post-change periods solely based on a statistical analysis is not sufficient. This selection is further justified based on physical characteristics of the watershed, and it is consistent with multiple studies that identified the mid to late 1990s as the period of major changes in the lake's watershed. For instance, Chaudhari et al. (2018) demonstrated that the impacts of human activities (e.g., dam constructions and the expansion of urban and agricultural lands) on the streamflow (Q) inflowing to the lake were amplified beginning 1999 (with the lowest annual average P within the period of 1979–2016), coinciding with a severe drought started in 1998, leading to a significant decrease in Q into the lake. Alborzi et al. (2018) have also demonstrated a significant decrease in Q into the lake during the early 2000s due to the drought period of 1998–2002 and increased withdrawal of surface water resources to meet the potable and agricultural water demands during this period. Due to the fact that the existing autocorrelation in monthly records could bias trend results, seasonal Kendall trends are also calculated to evaluate the overall trends.

4.2.1. Is there a potential link between the changes in WL, T, and P?

No overall long-term and short-term (both pre- and post-change) trends are found for climatic variables (P and T). While the strong seasonal and overall trends of WL for the pre-change period are increasing, it exhibits a strong decreasing trend, both seasonally and overall, during the post-change period. Due to the strength of the post-change WL trends, the long-term trends (seasonal and overall) are also decreasing, with a greater order of magnitude (i.e., Z_{MK} and Z_{SK}) for WL than the other hydro-climatic variables.

No trend is detected in P records across the time scales. Although increasing seasonal trends are apparent in the long-term and pre-

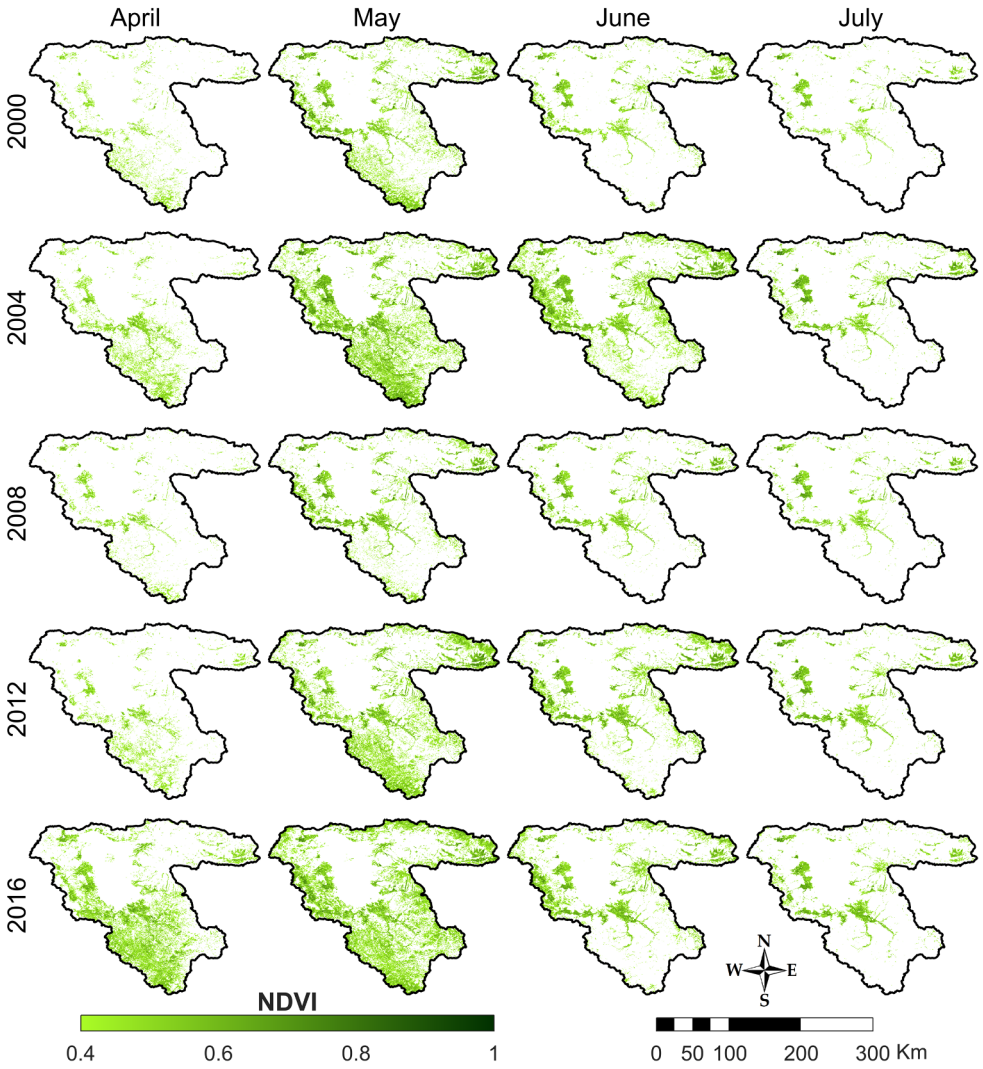

Fig. 8. Spatio-temporal variations of NDVI in the Lake Urmia watershed during April, May, June, and July based on MODIS NDVI.

change short-term T records, no trend is detected in the post-change period with severe declining trends in WL. These observations on P and T trends contradict the proposition that Lake Urmia has been subjected to lower P and higher T during the past two decades. That said, the possible association between WL fluctuations and variability in P and T is further investigated in the next section (4.3. Correlation Analysis).

4.2.2. Is there a link between the changes in WL and VC?

Although there is a positive seasonal trend in VC during both pre- and post-change periods, the post-change trend is stronger (a greater order of magnitude in terms of the trend test statistic Z_{sk}) due to the expansion of irrigation and agricultural activities (discussed in Section 4.4). Given the high correlation found in other studies between vegetation increase and increase in total evapotranspiration (ET) as well as the transpiration component in ET (Orth and Destouni, 2018), the positive and steeper trend in the post-change VC, compared to its pre-change trend, implies increased transpiration and associated total ET in this period, over which the overall P, T, and SM levels remain essentially stable. The observed increase in VC is also consistent with reports on expansion of agricultural lands and increased water withdrawal in the region (Ashraf et al., 2017; Chaudhari et al., 2018). As a consequence of fundamental water balance in the watershed—in analogy with similar previous findings, e.g., for the Aral Sea desiccation (Destouni et al., 2010)—increased ET (due to intensive or inefficient irrigation) under stable P and SM conditions means that runoff in the watershed and the associated discharge Q into the lake must have decreased in this period, leading to the observed WL decline by ~8 m (~50% of the maximum depth of the lake) between 1995 and 2016.

4.2.3. Trends in wet and dry spells

The hydro-climatic changes in the wet and dry months (May and July) were also examined for potential dominant seasonal variations (see Fig. 10).

As shown in Fig. 10, the overall trends in May (wet month) and July (dry month) records are similar to the short- and long-term trends in the mean monthly time series. While P, T, and SM either exhibit statistically non-significant or almost near-horizontal trends, WL has seasonal decreasing trends. Although the VC records for the dry month are not statistically significant, there is a dramatic increase during the wet month (which is also the growing season). This supports the potential link between WL decline and VC expansion, and the implication that ET has increased due to the increased VC in this month calling for further investigation of possible anthropogenic factors in the watershed driving the VC and associated ET increases. It also raises the question whether the required water for expansion of VC was supplied by over-exploitation of groundwater resources.

Overall, the wet and dry trend results also indicate that observed climatic changes (in terms of P and T) are not the likely dominant drivers of the WL change trend in both wet and dry months (May and July, respectively). The positive trend in WL in the years before 1995 is

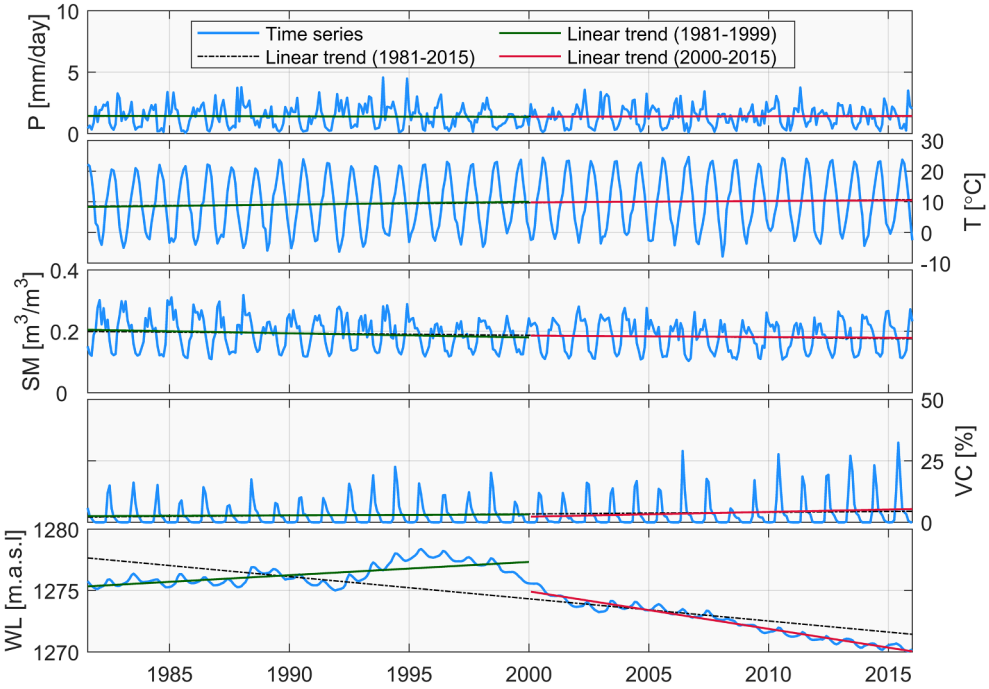

Fig. 9. Short- and long-term trends in hydro-climatic variables in the Lake Urmia watershed.

possibly due to high P events (Chaudhari et al., 2018), however (Jalili et al., 2015) showed that the positive trend of lake WL during 1966 and 1995 is not significant at a 95% confidence level. Further, even with an observed spike in P in May 1986, 2002, 2004, 2010, and 2013, WL decreased in these years.

It is noteworthy that WL in the lake is an integrated quantity. That is, WL fluctuations in a particular period (e.g., during May and July) are the integrated result of interactions between different hydro-climatic components of the lake system in the previous months. Therefore, a comprehensive comparison of the hydro-climate variables requires lagged correlation analysis between these variables and lake WL, as presented in Section 4.3. In addition, hydro-climate variables are subject to seasonal cycles. Therefore, the change-attribution analysis has also been carried out for the standardized anomalies (i.e., excluding the seasonal variations). In order to reduce the influence of seasonal cycles, long-term average and standard deviation of data for each month of the year are used as baseline and for standardization, respectively, in anomaly computations. Results of the change-attribution analysis of anomalies (see Figure S1 in Supplementary Materials) are consistent with those of the original data, which resolves the concern about the effects of seasonal variations in the hydro-climate and vegetation variables.

4.3. Correlation analysis

To further investigate the association between WL decline and changes in other hydro-climatic variables, correlation analysis is performed on the monthly averaged data, across the time series during 1981–2015. Long-term correlations are presented in Table 2. The results of all three correlation methods are consistent in terms of the degree of correlation (and their associated statistical significance) between hydro-climatic variables. Given the nonlinear and complex nature of interactions between different hydro-climatic processes, in addition to simultaneous correlation (lag time = 0), we also examine lagged correlations (1 to 5 months lag between the variables). For instance, time lags, particularly at the watershed scale, between P and VC and/or WL response can be expected (Herrmann et al., 2005; Wang et al., 2003). Therefore, here we only present the results for lags with the highest CCs in Table 2. VC lags five months behind P and SM, and WL lags three months behind P and four months behind T, SM, and VC, while no time lag is evident in correlations of other variables.

The highest short-term (pre- and post-change) correlations, comparing simultaneous and lagged CCs, are presented in Fig. 11. For the short-term correlations, only the Spearman CCs are presented and discussed as Spearman correlation can capture any monotonic relationship

Table 1
Mann-Kendall overall and seasonal Kendall trend statistics of hydro-climatic variables in the Lake Urmia watershed for short-term (pre-change and post-change) and long-term periods. Statistically significant values at p-value < 0.05 are indicated in bold.

Period	Method	Test Statistic	P	T	SM	VC	WL
Pre-change short-term (1981–1999)	Overall Mann-Kendall	Z_{MK}	−0.41	0.99	−1.82	0.45	**9.52**
		p-value	0.68	0.32	0.07	0.65	**0.00**
	Seasonal Kendall	Z_{SK}	0.16	**5.11**	**−3.14**	**2.44**	**9.37**
		p-value	0.87	**0.00**	**0.00**	**0.01**	**0.00**
Post-change short-term (2000–2015)	Overall Mann-Kendall	Z_{MK}	0.48	0.32	−0.66	0.97	**−18.09**
		p-value	0.63	0.75	0.51	0.33	**0.00**
	Seasonal Kendall	Z_{SK}	1.08	0.95	−0.56	**4.25**	**−17.93**
		p-value	0.28	0.34	0.58	**0.00**	**0.00**
Long-term (1981–2015)	Overall Mann-Kendall	Z_{MK}	0.26	1.68	**−2.60**	1.22	**−16.96**
		p-value	0.79	0.09	**0.01**	0.22	**0.00**
	Seasonal Kendall	Z_{SK}	1.00	**9.31**	**−6.06**	**4.72**	**−16.78**
		p-value	0.32	**0.00**	**0.00**	**0.00**	**0.00**

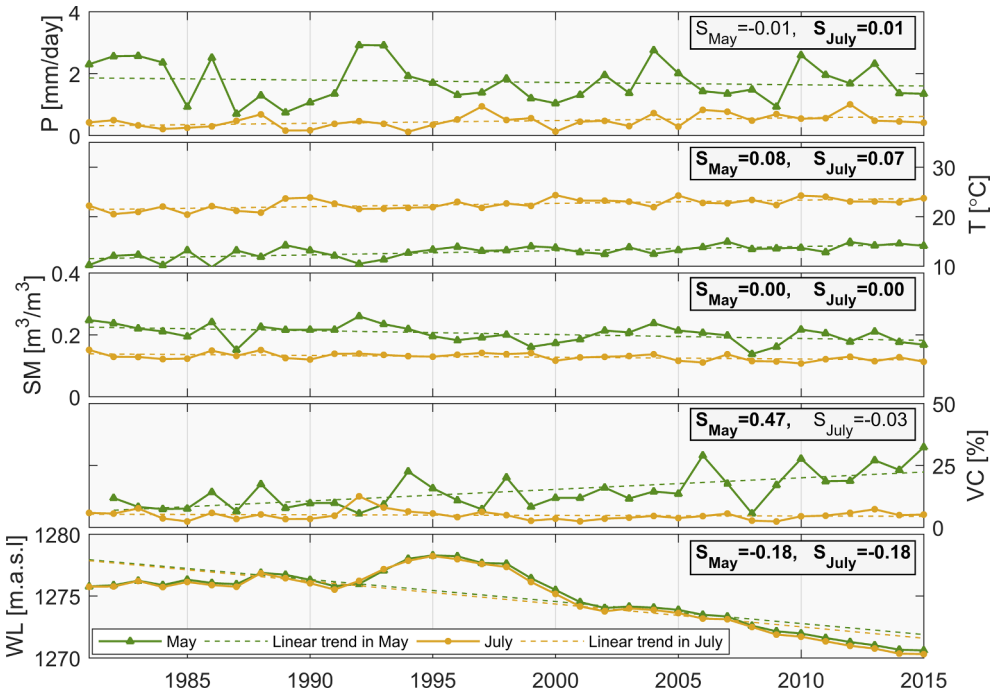

Fig. 10. Comparison of hydro-climatic trends in May (wet month) and July (dry month) during 1981–2015. S_{May} and S_{July} are the slopes of trends in May and July, respectively. Statistically significant slopes at *p*-value < 0.05 are shown in bold.

Table 2
Long-term CCs of hydro-climatic variables (upper triangular matrix), and the corresponding *p*-values in italics (lower triangular matrix). Statistically significant CC values at *p*-value < 0.05 are indicated in bold. The results of the lag times with the highest CCs are presented here.

Method	Test Statistic	Parameter	P	T	SM	VC	WL
Pearson	Coefficient	P	—	**-0.63**	**0.73**	**0.33**	0.08
		T	***0.00***	—	**-0.84**	**0.48**	**-0.14**
		SM	***0.00***	***0.00***	—	**0.53**	**0.16**
		VC	***0.00***	***0.00***	***0.00***	—	**-0.17**
	p-value	WL	*0.11*	***0.00***	***0.00***	***0.00***	—
Spearman	Coefficient	P	—	**-0.68**	**0.78**	**0.63**	0.10
		T	***0.00***	—	**-0.84**	**0.85**	**-0.18**
		SM	***0.00***	***0.00***	—	**0.80**	**0.19**
		VC	***0.00***	***0.00***	***0.00***	—	**-0.15**
	p-value	WL	*0.06*	***0.00***	***0.00***	***0.00***	—
Kendall	Coefficient	P	—	**-0.47**	**0.57**	**0.44**	0.06
		T	***0.00***	—	**-0.63**	**0.64**	**-0.13**
		SM	***0.00***	***0.00***	—	**0.61**	**0.13**
		VC	***0.00***	***0.00***	***0.00***	—	**-0.11**
	p-value	WL	*0.06*	***0.00***	***0.00***	***0.00***	—

(both linear and non-linear) between variables; unlike Pearson correlation that can only detect linear ones (Wilks, 2011). It should be further noted that non-monotonic associations between the hydro-climatic variables were not analyzed here, which can be an interesting extension of this study.

4.3.1. Could any (monotonic) relationship between WL decline and P and/or T variations be inferred?

Theoretically and under normal conditions, the lake WL goes up/down with higher/lower P, with both a direct input to the lake (P over the lake, with a smaller contribution) and an indirect one (P transformed into Q and eventually inflowing to the lake, with a higher contribution). Increase in T is directly correlated with higher ET rates, which in turn result in WL reduction. Therefore, some degree of monotonic relationship for WL-P and WL-T is expected. There is a strong P-T relationship, consistent in both pre- and post-change periods. During the pre-change period, there are weak and lagged monotonic relationships for WL-P (CC = 0.25 with a 3-month lag) and WL-T (CC = −0.29 with a 4-month lag), which are consistent with the expected physics of the lake WL fluctuations. However, during the post-change period there is no monotonic relationship for WL-P. That is, the relationship between P, as input to the lake, with WL, as the lake's response, has been disturbed. The strength of WL-T relationship during the post-change period is weakened by almost 40% (new CC = −0.17,

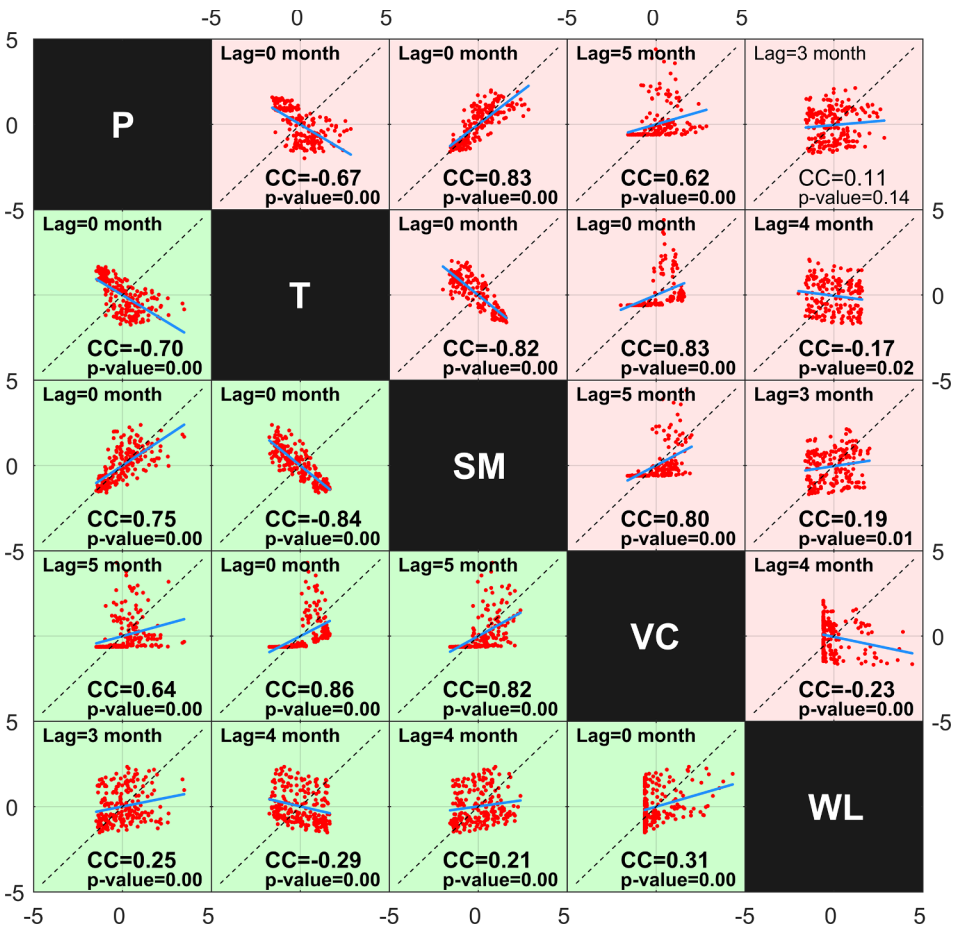

Fig. 11. Correlation-scatterplot matrix of monthly hydro-climatic data during the pre-change period (1981–1999; lower left in green) and post-change period (2000–2015; upper right in red). Statistically significant CC values at *p*-value < 0.05 are shown in bold. (For interpretation of the references to colour in this figure legend, the reader is referred to the web version of this article.)

with the similar lag time of 4 months) that reflects the possible impact of anthropogenic drivers of the lake WL during this period. The WL-T relationship in both wet and dry months is similar, but stronger (CC = −0.52), and consistent with pre- and post-change (see Fig. 12). Without an increasing trend recorded for T, it cannot be concluded that increased evaporation (the lake's only output flux) from the lake has driven the WL decline (Sima et al., 2013).

A slight change is seen in P-, T-, and SM-VC relationships from pre- to post-change periods. VC growth seems to be slightly more dependent on P, T, and SM in the pre-change period. One possible explanation for such a change could be the excessive withdrawal of groundwater resources—as a replacement for surface waters recharged by P–used for irrigation during the post-change period that is consistent with the observed groundwater level decline (Joodaki et al., 2014; Vaheddoost and Aksoy, 2018; Voss et al., 2013) in the watershed.

4.3.2. Could any (monotonic) relationship between WL decline and VC variations be inferred?

An interesting observation is the inversion of a direct and simultaneous association of the pre-change WL-VC (CC = 0.31) to an inverse and lagged association (CC = −0.23) during the post-change period. Although the strength of the relationship is moderate, the inversion of this relationship is an important observation. That is, during the pre-change period, changes in the VC did not negatively impact the WL; nonetheless, the dramatic expansion of VC during the post-change period (as shown in Figs. 8, 13, and 14) is associated with the WL decline. The seasonal associations for the dry and wet months during the post-change period further consolidates this observation. WL-VC exhibits a strong seasonal relationship (CC = −0.74) for both dry and wet months during the post-change period. The negative CC for WL-VC, signifying the negative effect of VC expansion on the lake WL, supports the conclusion that the ET increase, associated with increased VC, plays an important role in decreasing Q and discharge into the lake. In addition, Stone (2015) argued that farmers' shift to more water-demanding crops increased agricultural water demand and contributed to the shift in WL-VC relationship by reducing Q. The 4-month lag for the WL-VC relationship during the post-change period may correspond to a number of factors including the propagation time to the lake water deficit created at the surface by water use for vegetation growth and/or upstream reservoir operation policies, water storage for agricultural irrigation, and the differences in the seasonal cycles between these variables.

During 2000–2015 when WL in Lake Urmia has declined more than in any other time (since the 1960s), the WL-VC relationship is negative. Vegetated areas were extended—due to anthropogenic land-use change and agricultural land developments—in the watershed in this period, while the lake lost a significant amount of water. This inconsistency can be explained only by accounting for the amount of water used for agricultural activities in the watershed that increased VC at the expense of reducing lake inflows. This relationship is again consistent with increases in the transpiration component, and thereby the total ET.

4.4. Agricultural growth and associated land-water-use changes

As shown earlier, the VC and agriculture in the Lake Urmia watershed have increased in recent decades (Mehrian et al., 2016). In this section, a detailed assessment of historical changes in the VC based on MODIS NDVI is presented. Figs. 13 and 14 illustrate the changes in VC during the past 17 years in May. Histograms of NDVI frequency in the Lake Urmia watershed in May during 2001 to 2016 are shown in Fig. 13, with green bars for values above 0.4 classified as vegetation. Values ranging from 0.2 to 0.4 indicate a combination of soil, rock,

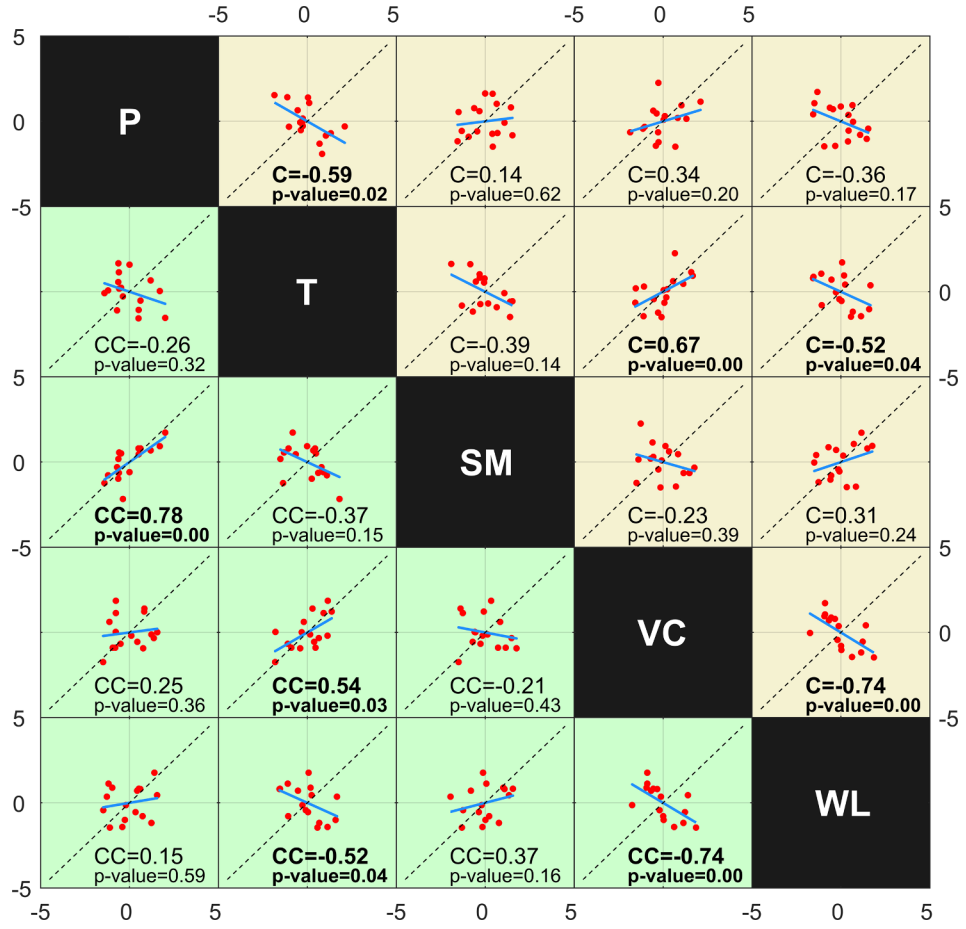

Fig. 12. Correlation-scatterplot matrix of the data in wet month May (lower left section in green) and dry month July (upper right section in beige) for the post-change period. (For interpretation of the references to colour in this figure legend, the reader is referred to the web version of this article.)

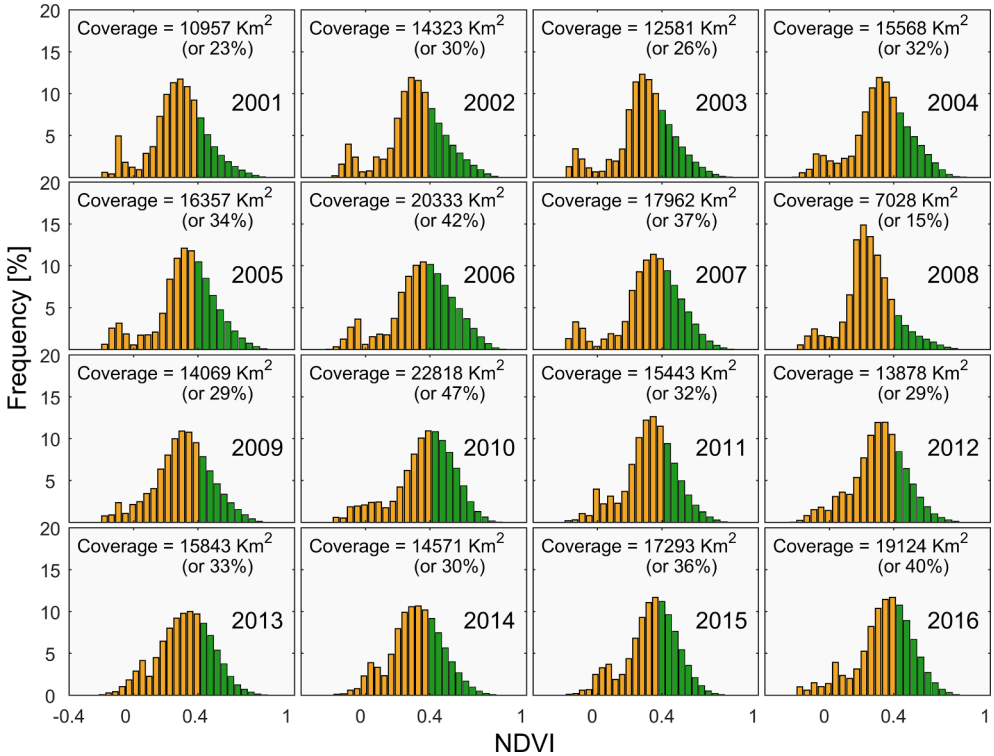

Fig. 13. Temporal variability of the histograms of NDVI frequency in the Lake Urmia watershed in May. Green bars show values above 0.4 that are classified as vegetation. (For interpretation of the references to colour in this figure legend, the reader is referred to the web version of this article.)

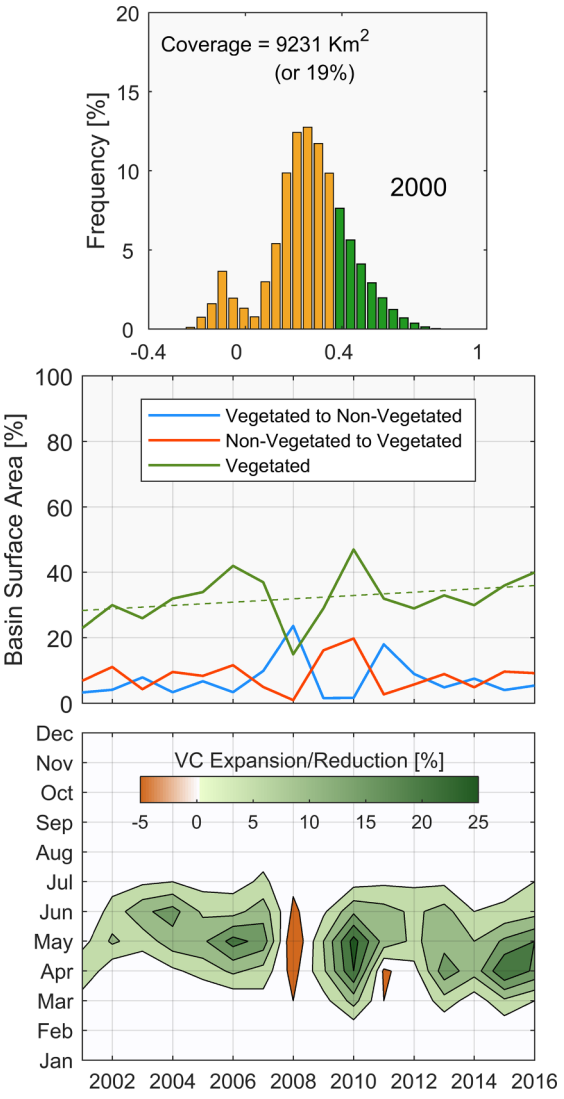

Fig. 14. Histogram of NDVI frequency in May 2000 (top), relative change in vegetation coverage (VC) in May of each year compared with the previous year (middle), and Change in VC in different months during 2001–2016 relative to VC in the corresponding month of the baseline year 2000 (bottom).

urban areas, and developed lands, and the range of −0.2 to 0.1 is associated with land covered with water (mostly the lake).

Fig. 14 (middle) illustrates relative annual changes in average NDVI values (based on MODIS data), as a measure of VC, in the wet month (May) during 2001–2016, i.e., the plot shows the ratio of the year-to-year changes (as percentage) in the vegetated area of the watershed in May over this period. The results show that VC in May was nearly doubled during the period 2000–2016. Moreover, Fig. 14 (bottom) illustrates that this major expansion in VC during 2010–2016 occurred in the March-July season (peaking in April-May) of each year, with almost no relative change in other months. Since the March-July season involves more intensive agricultural activities in the Lake Urmia watershed, sharp inter-annual variations and changes of VC in this season are likely associated with such activities.

VC increase can also be due to CO_2 enrichment; that is, the rise of atmospheric CO_2 concentration may lead to increased vegetation growth (Peel, 2009). However, available land cover classifications for the Lake Urmia watershed show that non-irrigated vegetated areas have increased only slightly between 1987 and 2016, while irrigated vegetated areas (cropland) have increased substantially during this period (Chaudhari et al., 2018). Therefore, it can be inferred that the CO_2 fertilization impact on VC increase is marginal, compared to the impact of agricultural and irrigation expansions. Regardless of whether or not VC expansion is CO_2-driven, increase in vegetation is associated with increased ET since vegetation transpires and therefore needs more water for its transpiration. This additional water use for transpiration affects to some degree (depending on the magnitude of vegetation increase and its water use for transpiration) the availability of remaining water in the watershed and the runoff to the lake, and thereby the WL in the lake.

Overall, the results indicate a substantial increase in VC, with associated transpiration and total ET increase (under stable T conditions), and resulting decrease in Q (under stable P and SM conditions) in the Lake Urmia watershed. The subsequent reduced water discharge into the lake, under aggressive land- and water-use changes required for the expansion of (irrigated) agriculture that has occurred in this watershed since the late 1990 s (Mehrian et al., 2016; Sigaroodi and Ebrahimi, 2010) can be therefore identified as the likely cause of the observed severe decline in the lake WL.

5. Conclusions

Understanding and distinguishing the atmospheric-climate and human-landscape drivers of major WL changes of (drying) lakes is a high research priority, particularly for water resources management and planning (Clites et al., 2014). These change drivers are also essential for management of other natural resources, given the strong inter-connection and inter-dependency of water resources, energy generation, and food production especially in transboundary basins such as Lake Urmia (Destouni et al., 2013; Engström et al., 2017; Jaramillo and Destouni, 2015; Keskinen et al., 2016; Madani and Khatami, 2015; Stevens and Madani, 2016; Tarroja et al., 2014). In developing a change-attribution approach for such WL changes, we have investigated available records of hydro-climatic and vegetation variables (P, T, SM, WL, and VC) for Lake Urmia and its watershed during the 1981–2015 period. The statistical analysis has identified the year 2000 as the point of major change in WL, leading to further analysis of the hydro-climatic and vegetation characteristics within the two short-term periods of pre-change (1981–1999) and post-change (2000–2015).

Given the stable conditions of P and T (i.e., no statistically significant trends) during both periods, we conclude that these atmospheric climatic changes cannot explain the dramatic decline of WL in Lake Urmia since 2000. Instead, the inversion of the WL-VC association—from a positive monotonic relationship in the pre-change period to a negative monotonic relationship in the post-change period—supports the hypothesis that regional human interventions (in terms of agricultural and associated irrigation expansions) are a *primary* cause of the lake desiccation. This hypothesis is further supported by the overall and seasonal analysis of vegetation dynamics and land-use changes over the Lake Urmia watershed.

Increased agricultural crop transpiration and thus total ET, associated with the human-driven increase in VC (inherently including irrigation, and water diversion and storage), leading to decreased runoff and thus Q from the watershed into the lake explains the dramatic WL decline in recent decades. The impact of VC expansion on water availability in the watershed and Lake Urmia itself may be further investigated based on additional data for changes in the total water balance of the watershed during the pre- and post-change periods, taking into account all main water fluxes and storage changes. The study results are consistent with studies of other parts of the world in indicating landscape changes in human land-use and water-use as main drivers of water resource changes (Destouni et al., 2013; Jaramillo and Destouni, 2015, 2014). Those studies have also shown that, additionally, atmospheric climate change (sustained changes in P and T) may intensify or dampen water changes, such as lake desiccation, relative to those driven by land/water-use changes; however, for the desiccation of Lake

Urmia, available observations do not provide conclusive evidence for T and P changes can be considered as the *primary* causes of the lake drying so far.

6. Declarations of interest

None.

Funding

This study was not supported by any public, commercial, or not-for-profit organization, and the authors did not receive any financial support to conduct this analysis.

Acknowledgments

The authors would like to thank Ali Hajimoradi, Head of Technical and Policy Division at Urmia Lake Restoration Program, for his kind assistance in sharing the lake water level data. The authors also thank René Orth and two other anonymous reviewers for their constructive feedback.

Appendix A. Supplementary data

Supplementary data to this article can be found online at https://doi.org/10.1016/j.jhydrol.2018.12.004.

References

Adler, R.F., Huffman, G.J., Chang, A., Ferraro, R., Xie, P.-P., Janowiak, J., Rudolf, B., Schneider, U., Curtis, S., Bolvin, D., Gruber, A., Susskind, J., Arkin, P., Nelkin, E., Adler, R.F., Huffman, G.J., Chang, A., Ferraro, R., Xie, P.-P., Janowiak, J., Rudolf, B., Schneider, U., Curtis, S., Bolvin, D., Gruber, A., Susskind, J., Arkin, P., Nelkin, E., 2003. The Version-2 Global Precipitation Climatology Project (GPCP) Monthly Precipitation Analysis (1979-Present). J. Hydrometeorol. 4, 1147–1167. https://doi.org/10.1175/1525-7541(2003) 004<1147:TVGPCP>2.0.CO;2.

AghaKouchak, A., Feldman, D., Hoerling, M., Huxman, T., Lund, J., 2015a. Water and climate: recognize anthropogenic drought. Nature 524, 409–411. https://doi.org/10.1038/524409a.

AghaKouchak, A., Norouzi, H., Madani, K., Mirchi, A., Azarderakhsh, M., Nazemi, A., Nasrollahi, N., Farahmand, A., Mehran, A., Hasanzadeh, E., 2015b. Aral Sea syndrome desiccates Lake Urmia: call for action. J. Great Lakes Res. https://doi.org/10.1016/j.jglr.2014.12.007.

Ahn, K.-H., Merwade, V., 2014. Quantifying the relative impact of climate and human activities on streamflow. J. Hydrol. 515, 257–266. https://doi.org/10.1016/j.jhydrol.2014.04.062.

Al-Damkhi, A.M., Abdul-Wahab, S.A., Al-Nafisi, A.S., 2009. On the need to reconsider water management in Kuwait. Clean Technol. Environ. Policy 11, 379–384. https://doi.org/10.1007/s10098-009-0201-z.

Alborzi, A., Mirchi, A., Moftakhari, H., Mallakpour, I., Alian, S., Nazemi, A., Hassanzadeh, E., Mazdiyasni, O., Ashraf, S., Madani, K., Norouzi, H., Azarderakhsh, M., Mehran, A., Sadegh, M., Castelletti, A., AghaKouchak, A., 2018. Climate-informed environmental inflows to revive a drying lake facing meteorological and anthropogenic droughts. Environ. Res. Lett. https://doi.org/10.1088/1748-9326/aad246.

Alemohammad, S.H., McColl, K.A., Konings, A.G., Entekhabi, D., Stoffelen, A., 2015. Characterization of precipitation product errors across the United States using multiplicative triple collocation. Hydrol. Earth Syst. Sci. 19, 3489–3503. https://doi.org/10.5194/hess-19-3489-2015.

Alizade Govarchin Ghale, Y., Altunkaynak, A., Unal, A., 2018. Investigation Anthropogenic Impacts and Climate Factors on Drying up of Urmia Lake using Water Budget and Drought Analysis. Water Resour. Manag. 32, 325–337. https://doi.org/10.1007/s11269-017-1812-5.

Amiri, V., Nakhaei, M., Lak, R., 2017. Using radon-222 and radium-226 isotopes to deduce the functioning of a coastal aquifer adjacent to a hypersaline lake in NW Iran. J. Asian Earth Sci. 147, 128–147. https://doi.org/10.1016/J.JSEAES.2017.07.015.

Amiri, V., Nakhaei, M., Lak, R., Kholghi, M., 2016. Geophysical, isotopic, and hydrogeochemical tools to identify potential impacts on coastal groundwater resources from Urmia hypersaline Lake, NW Iran. Environ. Sci. Pollut. Res. 23, 16738–16760. https://doi.org/10.1007/s11356-016-6859-y.

Ashouri, H., Hsu, K.-L., Sorooshian, S., Braithwaite, D.K., Knapp, K.R., Cecil, L.D., Nelson, B.R., Prat, O.P., Ashouri, H., Hsu, K.-L., Sorooshian, S., Braithwaite, D.K., Knapp, K.R., Cecil, L.D., Nelson, B.R., Prat, O.P., 2015. PERSIANN-CDR: Daily Precipitation Climate Data Record from Multisatellite Observations for Hydrological and Climate Studies. Bull. Am. Meteorol. Soc. 96, 69–83. https://doi.org/10.1175/BAMS-D-13-00068.1.

Ashraf, B., AghaKouchak, A., Alizadeh, A., Mousavi Baygi, M., Moftakhari, R.H., Mirchi, A., Anjileli, H., Madani, K., 2017. Quantifying Anthropogenic Stress on Groundwater Resources. Sci. Rep. 7, 12910. https://doi.org/10.1038/s41598-017-12877-4.

Baldwin, A.H., Egnotovich, M.S., Clarke, E., 2001. Hydrologic change and vegetation of tidal freshwater marshes: field, greenhouse, and seed-bank experiments. Wetlands 21, 519–531. https://doi.org/10.1672/0277-5212(2001) 021[0519:HCAVOT]2.0.CO;2.

Bari Abarghouei, H., Asadi Zarch, M.A., Dastorani, M.T., Kousari, M.R., Safari Zarch, M., 2011. The survey of climatic drought trend in Iran. Stoch. Environ. Res. Risk Assess. 25, 851–863. https://doi.org/10.1007/s00477-011-0491-7.

Berndtsson, R., Jebari, S., Hashemi, H., Wessels, J., 2016. Traditional irrigation techniques in MENA with focus on Tunisia. Hydrol. Sci. J. 02626667 (2016), 1165349. https://doi.org/10.1080/02626667.2016.1165349.

Bevan, A., 2013. Statistical Data Analysis for the Physical Sciences. Cambridge University Press, New York.

Burn, D.H., Hag Elnur, M.A., 2002. Detection of hydrologic trends and variability. J. Hydrol. 255, 107–122. https://doi.org/10.1016/S0022-1694(01)00514-5.

Chaudhari, S., Felfelani, F., Shin, S., Pokhrel, Y., 2018. Climate and anthropogenic contributions to the desiccation of the second largest saline lake in the twentieth century. J. Hydrol. 560, 342–353. https://doi.org/10.1016/J.JHYDROL.2018.03.034.

Clites, A.H., Smith, J.P., Hunter, T.S., Gronewold, A.D., 2014. Visualizing relationships between hydrology, climate, and water level fluctuations on Earth's largest system of lakes. J. Great Lakes Res. 40, 807–811. https://doi.org/10.1016/J.JGLR.2014.05.014.

Davtalab, R., Madani, K., Massah, A., Farajzadeh, M., 2014. Evaluating the Effects of Climate Change on Water Reliability in Iran's Karkheh River Basin, in: World Environmental and Water Resources Congress 2014. American Society of Civil Engineers, Reston, VA, pp. 2127–2135. https://doi.org/10.1061/9780784413548.212.

Davtalab, R., Mirchi, A., Khatami, S., Gyawali, R., Massah, A., Farajzadeh, M., Madani, K., 2017. Improving Continuous Hydrologic Modeling of Data-Poor River Basins Using Hydrologic Engineering Center's Hydrologic Modeling System: Case Study of Karkheh River Basin. J. Hydrol. Eng. 22, 5017011. https://doi.org/10.1061/(ASCE)HE.1943-5584.0001525.

Delbart, N., Kergoat, L., Le Toan, T., Lhermitte, J., Picard, G., 2005. Determination of phenological dates in boreal regions using normalized difference water index. Remote Sens. Environ. 97, 26–38. https://doi.org/10.1016/J.RSE.2005.03.011.

Delju, A.H., Ceylan, A., Piguet, E., Rebetez, M., 2013. Observed climate variability and change in Urmia Lake Basin, Iran. Theor. Appl. Climatol. 111, 285–296. https://doi.org/10.1007/s00704-012-0651-9.

Destouni, G., Asokan, S.M., Jarsjö, J., 2010. Inland hydro-climatic interaction: Effects of human water use on regional climate. Geophys. Res. Lett. 37, n/a-n/a. https://doi.org/10.1029/2010GL044153.

Destouni, G., Jaramillo, F., Prieto, C., 2013. Hydroclimatic shifts driven by human water use for food and energy production. Nat. Clim. Chang. 3, 213–217. https://doi.org/10.1038/nclimate1719.

Didan, K., 2015. MOD13Q1 MODIS/Terra Vegetation Indices 16-Day L3 Global 250m SIN Grid V006. https://doi.org/10.5067/MODIS/MOD13Q1.006.

Douglas, E.M., Vogel, R.M., Kroll, C.N., 2000. Trends in floods and low flows in the United States: impact of spatial correlation. J. Hydrol. 240, 90–105.

Draper, C., Reichle, R., de Jeu, R., Naeimi, V., Parinussa, R., Wagner, W., 2013. Estimating root mean square errors in remotely sensed soil moisture over continental scale domains. Remote Sens. Environ. 137, 288–298. https://doi.org/10.1016/j.rse.2013.06.013.

Engström, R.E., Howells, M., Destouni, G., Bhatt, V., Bazilian, M., Rogner, H.-H., 2017. Connecting the resource nexus to basic urban service provision – with a focus on water-energy interactions in New York City. Sustain. Cities Soc. 31, 83–94. https://doi.org/10.1016/J.SCS.2017.02.007.

Fan, X., Shi, C., Zhou, Y., Shao, W., 2012. Sediment rating curves in the Ningxia-Inner Mongolia reaches of the upper Yellow River and their implications. Quat. Int. 282, 152–162. https://doi.org/10.1016/j.quaint.2012.04.044.

Fan, Y., van den Dool, H., 2008. A global monthly land surface air temperature analysis for 1948-present. J. Geophys. Res. Atmos. 113. https://doi.org/10.1029/2007JD008470.

Farajzadeh, J., Fakheri Fard, A., Lotfi, S., 2014. Modeling of monthly rainfall and runoff of Urmia lake basin using "feed-forward neural network" and "time series analysis" model. Water Resour. Ind. 7–8, 38–48. https://doi.org/10.1016/j.wri.2014.10.003.

Fathian, F., Morid, S., Kahya, E., 2015. Identification of trends in hydrological and climatic variables in Urmia Lake basin, Iran. Theor. Appl. Climatol. 119, 443–464. https://doi.org/10.1007/s00704-014-1120-4.

Fazel, N., Berndtsson, R., Uvo, C.B., Madani, K., Kløve, B., 2017. Regionalization of precipitation characteristics in Iran's Lake Urmia basin. Theor. Appl. Climatol. 1–11. https://doi.org/10.1007/s00704-017-2090-0.

Felfelani, F., Wada, Y., Longuevergne, L., Pokhrel, Y.N., 2017. Natural and human-induced terrestrial water storage change: a global analysis using hydrological models and GRACE. J. Hydrol. 553, 105–118. https://doi.org/10.1016/J.JHYDROL.2017.07.048.

Gessner, U., Naeimi, V., Klein, I., Kuenzer, C., Klein, D., Dech, S., 2013. The relationship between precipitation anomalies and satellite-derived vegetation activity in Central Asia. Glob. Planet. Change 110, 74–87. https://doi.org/10.1016/j.gloplacha.2012.09.007.

Gohari, A., Eslamian, S., Mirchi, A., Abedi-Koupaei, J., Massah Bavani, A., Madani, K., 2013. Water transfer as a solution to water shortage: a fix that can Backfire. J. Hydrol. 491, 23–39. https://doi.org/10.1016/J.JHYDROL.2013.03.021.

Golian, S., Mazdiyasni, O., AghaKouchak, A., 2015. Trends in meteorological and agricultural droughts in Iran. Theor. Appl. Climatol. 119, 679–688. https://doi.org/10.1007/s00704-014-1139-6.

Hashemi, H., 2015. Climate Change and the Future of Water Management in Iran. Middle

East Crit. 24, 307–323. https://doi.org/10.1080/19436149.2015.1046706.
Hashemi, H., Uvo, C.B., Berndtsson, R., 2015. Coupled modeling approach to assess climate change impacts on groundwater recharge and adaptation in arid areas. Hydrol. Earth Syst. Sci. 19, 4165–4181. https://doi.org/10.5194/hess-19-4165-2015.
Hassanzadeh, E., Zarghami, M., Hassanzadeh, Y., 2012. Determining the Main Factors in Declining the Urmia Lake Level by Using System Dynamics Modeling. Water Resour. Manag. 26, 129–145. https://doi.org/10.1007/s11269-011-9909-8.
Herrmann, S.M., Anyamba, A., Tucker, C.J., 2005. Recent trends in vegetation dynamics in the African Sahel and their relationship to climate. Glob. Environ. Chang. 15, 394–404. https://doi.org/10.1016/j.gloenvcha.2005.08.004.
Hirsch, R.M., Slack, J.R., 1984. A Nonparametric Trend Test for Seasonal Data With Serial Dependence. Water Resour. Res. 20, 727–732. https://doi.org/10.1029/WR020i006p00727.
House, A.R., Thompson, J.R., Acreman, M.C., 2016. Projecting impacts of climate change on hydrological conditions and biotic responses in a chalk valley riparian wetland. J. Hydrol. 534, 178–192. https://doi.org/10.1016/j.jhydrol.2016.01.004.
Huete, A., Didan, K., Miura, T., Rodriguez, E., Gao, X., Ferreira, L., 2002. Overview of the radiometric and biophysical performance of the MODIS vegetation indices. Remote Sens. Environ. 83, 195–213. https://doi.org/10.1016/S0034-4257(02)00096-2.
IPCC, 2014. Climate Change 2014: Synthesis Report. Contribution of Working Groups I, II and III to the Fifth Assessment Report of the Intergovernmental Panel on Climate Change [Core Writing Team, R.K. Pachauri and L.A. Meyer (eds.)]. IPCC, Geneva, Switzerland, p. 151.
Izady, A., Davary, K., Alizadeh, A., Ghahraman, B., Sadeghi, M., Moghaddamnia, A., 2012. Application of "panel-data" modeling to predict groundwater levels in the Neishaboor Plain, Iran. Hydrogeol. J. 20, 435–447. https://doi.org/10.1007/s10040-011-0814-2.
Jalili, S., Hamidi, S.A., Ghanbari, R.N., 2015. Climate variability and anthropogenic effects on Lake Urmia water level fluctuations, northwestern Iran. Hydrol. Sci. J. 6667, 150527103244004. https://doi.org/10.1080/02626667.2015.1036757.
Jalili, S., Kirchner, I., Livingstone, D.M., Morid, S., 2012. The influence of large-scale atmospheric circulation weather types on variations in the water level of Lake Urmia. Iran. Int. J. Climatol. 32, 1990–1996. https://doi.org/10.1002/joc.2422.
Jamali, S., Abrishamchi, A., Madani, K., 2013. Climate Change and Hydropower Planning in the Middle East: implications for Iran's Karkheh Hydropower Systems. J. Energy Eng. 139, 153–160. https://doi.org/10.1061/(ASCE)EY.1943-7897.0000115.
Jaramillo, F., Destouni, G., 2015. Comment on "Planetary boundaries: guiding human development on a changing planet". Science 348, 1217. https://doi.org/10.1126/science.aaa9629.
Jaramillo, F., Destouni, G., 2014. Developing water change spectra and distinguishing change drivers worldwide. Geophys. Res. Lett. 41, 8377–8386. https://doi.org/10.1002/2014GL061848.
Joodaki, G., Wahr, J., Swenson, S., 2014. Estimating the human contribution to groundwater depletion in the Middle East, from GRACE data, land surface models, and well observations. Water Resour. Res. 50, 2679–2692. https://doi.org/10.1002/2013WR014633.
Karbassi, A., Bidhendi, G.N., Pejman, A., Bidhendi, M.E., 2010. Environmental impacts of desalination on the ecology of Lake Urmia. J. Great Lakes Res. 36, 419–424. https://doi.org/10.1016/j.jglr.2010.06.004.
Kendall, M.G., Maurice, G., 1970. Rank Correlation Methods, 4th ed. Griffin, London.
Kendall, M.G., Maurice, G., Gibbons, J.D., 1990. Rank correlation methods. E. Arnold.
Keskinen, M., Guillaume, J., Kattelus, M., Porkka, M., Räsänen, T., Varis, O., Keskinen, M., Guillaume, J.H.A., Kattelus, M., Porkka, M., Räsänen, T.A., Varis, O., 2016. The Water-Energy-Food Nexus and the Transboundary Context: Insights from Large Asian Rivers. Water 8, 193. https://doi.org/10.3390/w8050193.
Khalyani, A.H., Mayer, A.L., Norman, E.S., 2014. Water Flows Toward Power: Socioecological Degradation of Lake Urmia, Iran. Soc. Nat. Resour. 27, 759–767. https://doi.org/10.1080/08941920.2014.905890.
Khatami, S., 2013. Nonlinear Chaotic and Trend Analyses of Water Level at Urmia Lake, Iran. Nonlinear Chaotic Trend Anal. Water Lev. Urmia Lake, Iran. M.Sc. Thesis Rep. TVVR-13/5012, ISSN1101–9824. Lund University, Lund, Sweden.
Khatami, S., Berndtsson, R., 2013. Urmia Lake watershed restoration in Iran: short- and long-term perspectives, in: Proceedings of the 6th International Perspective on Water Resources & the Environment (IPWE). Izmir, Turkey.
Khatami, S., Berndtsson, R., 2012. Integrated Watershed Management to Save the UNESCO Biosphere Reserve Lake Urmia, Iran, in: AWRA Annual Water Resources Conference. November 12-15, Jacksonville, Florida.
Khazaei, B., Hosseini, S.M., 2015. Improving the performance of water balance equation using fuzzy logic approach. J. Hydrol. 524, 538–548. https://doi.org/10.1016/j.jhydrol.2015.02.047.
Khazaei, B., Khatami, S., Rashidi, L., Madani, K., 2016. Hydro-climatic Investigation of Lake Urmia Shrinkage using Remote Sensing, in: American Geophysical Union 2016 Fall Meeting. San Francisco, Calif., 12-16 Dec.
Khazaei, B., Wu, C., 2018. Estimation of Vegetation Coverage Based on Seasonal Variabilities in MODIS-Based Vegetation Indices, in: World Environmental and Water Resources Congress 2018. American Society of Civil Engineers, Reston, VA, pp. 11–20. https://doi.org/10.1061/9780784481400.002.
Khoshtinat, S., Alami, M.T., Nezhad, B.A., 2015. Quantitative Effects Influencing Factors in the Urmia Lake Water Level Changes Using a System Dynamics Model 7, 861–870.
Khosravi, F., Jha-Thakur, U., Fischer, T.B., 2018. The role of environmental assessment (EA) in Iranian water management. Impact Assess. Proj. Apprais. 1–14. https://doi.org/10.1080/14615517.2018.1526998.
Kustas, W.P., Daughtry, C.S.T., Van Oevelen, P.J., 1993. Analytical treatment of the relationships between soil heat flux/net radiation ratio and vegetation indices. Remote Sens. Environ. 46, 319–330. https://doi.org/10.1016/0034-4257(93)90052-Y.
Liu, Y.Y., Dorigo, W.A., Parinussa, R.M., de Jeu, R.A.M., Wagner, W., McCabe, M.F., Evans, J.P., van Dijk, A.I.J.M., 2012. Trend-preserving blending of passive and active microwave soil moisture retrievals. Remote Sens. Environ. 123, 280–297. https://doi.org/10.1016/j.rse.2012.03.014.
Liu, Y.Y., Parinussa, R.M., Dorigo, W.A., De Jeu, R.A.M., Wagner, W., van Dijk, A.I.J.M., McCabe, M.F., Evans, J.P., 2011. Developing an improved soil moisture dataset by blending passive and active microwave satellite-based retrievals. Hydrol. Earth Syst. Sci. 15, 425–436. https://doi.org/10.5194/hess-15-425-2011.
Madani, K., 2014. Water management in Iran: what is causing the looming crisis? J. Environ. Stud. Sci. 4, 315–328. https://doi.org/10.1007/s13412-014-0182-z.
Madani, K., AghaKouchak, A., Mirchi, A., 2016. Iran's Socio-economic Drought: Challenges of a Water-Bankrupt Nation. Iran. Stud. 49, 997–1016. https://doi.org/10.1080/00210862.2016.1259286.
Madani, K., Khatami, S., 2015. Water for Energy: Inconsistent Assessment Standards and Inability to Judge Properly. Curr. Sustain. Energy Reports 2, 10–16. https://doi.org/10.1007/s40518-014-0022-5.
Mann, H.B., 1945. Nonparametric Tests Against Trend. Econometrica 13, 245. https://doi.org/10.2307/1907187.
Marjani, A., Jamali, M., 2014. Role of exchange flow in salt water balance of Urmia Lake. Dyn. Atmos. Ocean. 65, 1–16. https://doi.org/10.1016/j.dynatmoce.2013.10.001.
McColl, K.A., Vogelzang, J., Konings, A.G., Entekhabi, D., Piles, M., Stoffelen, A., 2014. Extended triple collocation: estimating errors and correlation coefficients with respect to an unknown target. Geophys. Res. Lett. 41, 6229–6236. https://doi.org/10.1002/2014GL061322.
Mehran, A., AghaKouchak, A., Nakhjiri, N., Stewardson, M.J., Peel, M.C., Phillips, T.J., Wada, Y., Ravalico, J.K., 2017. Compounding Impacts of Human-Induced Water Stress and Climate Change on Water Availability. Sci. Rep. 7, 6282. https://doi.org/10.1038/s41598-017-06765-0.
Mehran, A., Mazdiyasni, O., AghaKouchak, A., 2015. A hybrid framework for assessing socioeconomic drought: linking climate variability, local resilience, and demand. J. Geophys. Res. Atmos. 120, 7520–7533. https://doi.org/10.1002/2015JD023147.
Mehrian, M.R., Hernandez, R.P., Yavari, A.R., Faryadi, S., Salehi, E., 2016. Investigating the causality of changes in the landscape pattern of Lake Urmia basin, Iran using remote sensing and time series analysis. Environ. Monit. Assess. 188, 462. https://doi.org/10.1007/s10661-016-5456-3.
Mesgaran, M.B., Madani, K., Hashemi, H., Azadi, P., 2017. Iran's Land Suitability for Agriculture. Sci. Rep. 7, 7670. https://doi.org/10.1038/s41598-017-08066-y.
Mohan, C., Western, A.W., Wei, Y., Saft, M., 2018. Predicting groundwater recharge for varying land cover and climate conditions – a global meta-study. Hydrol. Earth Syst. Sci. 22, 2689–2703. https://doi.org/10.5194/hess-22-2689-2018.
NASA, 2017. Clouds and the Earth's Radiant Energy System (CERES) [WWW Document]. accessed 5.27.18. https://ceres.larc.nasa.gov/index.php.
NASA, 2014a. Vegetation Indices 16-Day L3 Global 250m (MOD13Q1) [WWW Document]. accessed 5.26.16. https://lpdaac.usgs.gov/dataset_discovery/modis/modis_products_table/mod13q1.
NASA, 2014b. AVHRR NDVI3g [WWW Document]. accessed 5.29.18. https://nex.nasa.gov/nex/projects/1349/.
NASA, 2012. NASA/GEWEX SRB [WWW Document]. accessed 5.26.18. https://eosweb.larc.nasa.gov/project/srb/srb_table.
Natural Earth Map Data. Made with Natural Earth. Free vector and raster map data @ naturalearthdata.com. [WWW Document]. URL http://www.naturalearthdata.com/about/terms-of-use/ (accessed 2.10.18).
Nemani, R., Running, S., 1997. Land cover characterization using multitemporal red, near-IR, and thermal-IR data from NOAA/AVHRR. Ecol. Appl. 7, 79–90. https://doi.org/10.1890/1051-0761(1997) 007[0079:LCCUMR]2.0.CO;2.
NOAA, 2016a. NOAA CPC Merged Analysis of Precipitation (CMAP) [WWW Document]. URL https://www.esrl.noaa.gov/psd/data/gridded/data.cmap.html.
NOAA, 2016b. NOAA GHCN_CAMS Land Temperature Analysis [WWW Document]. URL https://www.esrl.noaa.gov/psd/data/gridded/data.ghcncams.html.
Orth, R., Destouni, G., 2018. Drought reduces blue-water fluxes more strongly than green-water fluxes in Europe. Nat. Commun. 9, 3602. https://doi.org/10.1038/s41467-018-06013-7.
Orth, R., Seneviratne, S.I., 2015. Introduction of a simple-model-based land surface dataset for Europe. Environ. Res. Lett. 10, 44012. https://doi.org/10.1088/1748-9326/10/4/044012.
Pachauri, R.K., Meyer, L.A., 2014. IPCC, 2014: Climate Change 2014: Synthesis Report. Contribution of Working Groups I, II and III to the Fifth Assessment Report of the Intergovernmental Panel on Climate Change 1–151.
Parinussa, R.M., Holmes, T.R.H., Yilmaz, M.T., Crow, W.T., 2011. The impact of land surface temperature on soil moisture anomaly detection from passive microwave observations. Hydrol. Earth Syst. Sci. 15, 3135–3151. https://doi.org/10.5194/hess-15-3135-2011.
Peel, M.C., 2009. Hydrology: catchment vegetation and runoff. Prog. Phys. Geogr. 33, 837–844. https://doi.org/10.1177/0309133309350122.
Pettitt, A., 1979. A non-parametric approach to the change-point problem. Appl. Stat.
Piao, S., Mohammat, A., Fang, J., Cai, Q., Feng, J., 2006. NDVI-based increase in growth of temperate grasslands and its responses to climate changes in China. Glob. Environ. Chang. 16, 340–348. https://doi.org/10.1016/j.gloenvcha.2006.02.002.
Pinzon, J., Tucker, C., 2014. A Non-Stationary 1981–2012 AVHRR NDVI3g Time Series. Remote Sens. 6, 6929–6960. https://doi.org/10.3390/rs6086929.
Pokhrel, Y.N., Felfelani, F., Shin, S., Yamada, T.J., Satoh, Y., 2017. Modeling large-scale human alteration of land surface hydrology and climate. Geosci. Lett. 4, 10. https://doi.org/10.1186/s40562-017-0076-5.
Ratheesh, S., Mankad, B., Basu, S., Kumar, R., Sharma, R., 2013. Assessment of Satellite-Derived Sea Surface Salinity in the Indian Ocean. IEEE Geosci. Remote Sens. Lett. 10, 428–431. https://doi.org/10.1109/LGRS.2012.2207943.
Ratner, B., 2009. The correlation coefficient: its values range between +1/−1, or do

they? J. Targeting Meas. Anal. Mark. 17, 139–142. https://doi.org/10.1057/jt.2009.5.
Rodell, M., Famiglietti, J.S., Wiese, D.N., Reager, J.T., Beaudoing, H.K., Landerer, F.W., Lo, M.-H., 2018. Emerging trends in global freshwater availability. Nature 557, 651–659. https://doi.org/10.1038/s41586-018-0123-1.
Roebeling, R.A., Wolters, E.L.A., Meirink, J.F., Leijnse, H., Roebeling, R.A., Wolters, E.L.A., Meirink, J.F., Leijnse, H., 2012. Triple Collocation of Summer Precipitation Retrievals from SEVIRI over Europe with Gridded Rain Gauge and Weather Radar Data. J. Hydrometeorol. 13, 1552–1566. https://doi.org/10.1175/JHM-D-11-089.1.
Rougé, C., Ge, Y., Cai, X., 2013. Detecting gradual and abrupt changes in hydrological records. Adv. Water Resour. 53, 33–44. https://doi.org/10.1016/j.advwatres.2012.09.008.
Rouse, J.W., J., Haas, R.H., Schell, J.A., Deering, D.W., 1974. Monitoring Vegetation Systems in the Great Plains with Erts. Third Earth Resour. Technol. Satell. Symp. Vol. I Tech. Present. NASA SP-351, Compil. Ed. by Stanley C. Freden, Enrico P. Merc. Margaret A. Becker, 1994 pages, Publ. by NASA, Washington, D.C., 1974, pp. 309–351, 309.
Schultz, M., Clevers, J.G.P.W., Carter, S., Verbesselt, J., Avitabile, V., Quang, H.V., Herold, M., 2016. Performance of vegetation indices from Landsat time series in deforestation monitoring. Int. J. Appl. Earth Obs. Geoinf. 52, 318–327. https://doi.org/10.1016/j.jag.2016.06.020.
Sigaroodi, S.K., Ebrahimi, S., 2010. Effects of land use change on surface water regime (case study Orumieh Lake of Iran). Procedia Environ. Sci. 2, 256–261. https://doi.org/10.1016/j.proenv.2010.10.031.
Sima, S., Ahmadalipour, A., Tajrishy, M., 2013. Mapping surface temperature in a hypersaline lake and investigating the effect of temperature distribution on the lake evaporation. Remote Sens. Environ. 136, 374–385. https://doi.org/10.1016/J.RSE.2013.05.014.
Stevens, T., Madani, K., 2016. Future climate impacts on maize farming and food security in Malawi. Sci. Rep. 6, 36241. https://doi.org/10.1038/srep36241.
Stoffelen, A., 1998. Toward the true near-surface wind speed: Error modeling and calibration using triple collocation. J. Geophys. Res. Ocean. 103, 7755–7766. https://doi.org/10.1029/97JC03180.
Stone, R., 2015. Saving iran's great salt lake. Science (80-.). 349, 1044–1046.
Tarroja, B., AghaKouchak, A., Sobhani, R., Feldman, D., Jiang, S., Samuelsen, S., 2014. Evaluating options for Balancing the Water-Electricity Nexus in California: Part 1 – Securing Water Availability. Sci. Total Environ. 497–498, 697–710. https://doi.org/10.1016/J.SCITOTENV.2014.06.060.
Tian, Y., Huffman, G.J., Adler, R.F., Tang, L., Sapiano, M., Maggioni, V., Wu, H., 2013. Modeling errors in daily precipitation measurements: Additive or multiplicative? Geophys. Res. Lett 40. https://doi.org/10.1002/grl.50320.
Tillack, A., Clasen, A., Kleinschmit, B., Förster, M., 2014. Estimation of the seasonal leaf area index in an alluvial forest using high-resolution satellite-based vegetation indices. Remote Sens. Environ. 141, 52–63. https://doi.org/10.1016/j.rse.2013.10.018.
Torabi Haghighi, A., Fazel, N., Hekmatzadeh, A.A., Klöve, B., 2018. Analysis of Effective Environmental Flow Release Strategies for Lake Urmia Restoration. Water Resour. Manag. 32, 3595–3609. https://doi.org/10.1007/s11269-018-2008-3.
Tourian, M.J., Elmi, O., Chen, Q., Devaraju, B., Roohi, S., Sneeuw, N., 2015. A spaceborne multisensor approach to monitor the desiccation of Lake Urmia in Iran. Remote Sens. Environ. 156, 349–360. https://doi.org/10.1016/j.rse.2014.10.006.
Tucker, C.J., Molly, J.E.P., Brown, E., Slayback, D.A., Pak, E.W., Mahoney, R., Vermote, E.F., 2005. An extended AVHRR 8-kni NDVI dataset compatible with MODIS and SPOT vegetation NDVI data. Int. J. Remote Sens. 26, 4485–4498.
UNEP & GEAS, 2012. The Drying of Iran's Lake Urmia and its Environmental Consequences. Environ. Dev. 2, 128–137.
USDA, 2017. Global Reservoirs/Lakes (G-REALM) [WWW Document]. accessed 5.18.17. https://www.pecad.fas.usda.gov/cropexplorer/global_reservoir/.
Vaheddoost, B., Aksoy, H., 2018. Interaction of groundwater with Lake Urmia in Iran. Hydrol. Process. 32, 3283–3295. https://doi.org/10.1002/hyp.13263.
Vaheddoost, B., Aksoy, H., 2017. Structural characteristics of annual precipitation in Lake Urmia basin. Theor. Appl. Climatol. 128, 919–932. https://doi.org/10.1007/s00704-016-1748-3.
Villarini, G., Serinaldi, F., Smith, J.A., Krajewski, W.F., 2009. On the stationarity of annual flood peaks in the continental United States during the 20th century. Water Resour. Res. 45. https://doi.org/10.1029/2008WR007645.
Viña, A., Gitelson, A.A., Nguy-Robertson, A.L., Peng, Y., 2011. Comparison of different vegetation indices for the remote assessment of green leaf area index of crops. Remote Sens. Environ. 115, 3468–3478. https://doi.org/10.1016/j.rse.2011.08.010.
Vörösmarty, C.J., McIntyre, P.B., Gessner, M.O., Dudgeon, D., Prusevich, A., Green, P., Glidden, S., Bunn, S.E., Sullivan, C.A., Liermann, C.R., Davies, P.M., 2010. Global threats to human water security and river biodiversity. Nature 467, 555–561. https://doi.org/10.1038/nature09440.
Voss, K.A., Famiglietti, J.S., Lo, M., de Linage, C., Rodell, M., Swenson, S.C., 2013. Groundwater depletion in the Middle East from GRACE with implications for transboundary water management in the Tigris-Euphrates-Western Iran region. Water Resour. Res. 49, 904–914. https://doi.org/10.1002/wrcr.20078.
Wagner, W., Dorigo, W., de Jeu, R., Fernandez, D., Benveniste, J., Haas, E., Ertl, M., 2012. Fusion of active and passive microwave observations to create an essential climate variable data record on soil moisture. ISPRS Ann Photogramm. Remote Sens. Spat, Inf. Sci. I-7, 315–321. https://doi.org/10.5194/ISPRSANNALS-I-7-315-2012.
Wang, J., Rich, P.M., Price, K.P., 2003. Temporal responses of NDVI to precipitation and temperature in the central Great Plains. USA 24, 2345–2364. https://doi.org/10.1080/01431160210154812.
Wasserstein, R.L., Lazar, N.A., 2016. The ASA's Statement on p -Values: Context, Process, and Purpose. Am. Stat. 70, 129–133. https://doi.org/10.1080/00031305.2016.1154108.
Weier, J., Herring, D., 2000. Measuring Vegetation (NDVI & EVI) : Feature Articles [WWW Document]. URL http://earthobservatory.nasa.gov/Features/MeasuringVegetation/ (accessed 5.26.16).
Wilks, D.S., 2011. Statistical methods in the atmospheric sciences. Academic Press.
Yao, H., Shi, C., Shao, W., Bai, J., Yang, H., 2015. Impacts of Climate Change and Human Activities on Runoff and Sediment Load of the Xiliugou Basin in the Upper Yellow River. Adv. Meteorol. 2015, 1–12. https://doi.org/10.1155/2015/481713.
Zeinoddini, M., Tofighi, M.A., Vafaee, F., 2009. Evaluation of dike-type causeway impacts on the flow and salinity regimes in Urmia Lake. Iran. J. Great Lakes Res. 35, 13–22. https://doi.org/10.1016/j.jglr.2008.08.001.
Zoljoodi, M., Didevarasl, A., 2014. Water-Level Fluctuations of Urmia Lake: Relationship with the Long-Term Changes of Meteorological Variables (Solutions for Water-Crisis Management in Urmia Lake Basin). Atmos. Clim. Sci. 4, 358–368. https://doi.org/10.4236/acs.2014.43036.
Zribi, M., Paris Anguela, T., Duchemin, B., Lili, Z., Wagner, W., Hasenauer, S., Chehbouni, A., 2010. Relationship between soil moisture and vegetation in the Kairouan plain region of Tunisia using low spatial resolution satellite data. Water Resour. Res. 46. https://doi.org/10.1029/2009WR008196.